Applied and Environmental Microbiology, Oct. 2004, p. 6098–6112 Vol. 70, No. 10
0099-2240/04/$08.00+0 DOI: 10.1128/AEM.70.10.6098–6112.2004

Transcriptional Analysis of Biofilm Formation Processes in the Anaerobic, Hyperthermophilic Bacterium *Thermotoga maritima*

Marybeth A. Pysz,† Shannon B. Conners, Clemente I. Montero, Keith R. Shockley, Matthew R. Johnson, Donald E. Ward,‡ and Robert M. Kelly*

Department of Chemical Engineering, North Carolina State University, Raleigh, North Carolina

Received 24 February 2004/Accepted 2 April 2004

***Thermotoga maritima*, a fermentative, anaerobic, hyperthermophilic bacterium, was found to attach to bioreactor glass walls, nylon mesh, and polycarbonate filters during chemostat cultivation on maltose-based media at 80°C. A whole-genome cDNA microarray was used to examine differential expression patterns between biofilm and planktonic populations. Mixed-model statistical analysis revealed differential expression (twofold or more) of 114 open reading frames in sessile cells (6% of the genome), over a third of which were initially annotated as hypothetical proteins in the *T. maritima* genome. Among the previously annotated genes in the *T. maritima* genome, which showed expression changes during biofilm growth, were several that corresponded to biofilm formation genes identified in mesophilic bacteria (i.e., *Pseudomonas* species, *Escherichia coli*, and *Staphylococcus epidermidis*). Most notably, *T. maritima* biofilm-bound cells exhibited increased transcription of genes involved in iron and sulfur transport, as well as in biosynthesis of cysteine, thiamine, NAD, and isoprenoid side chains of quinones. These findings were all consistent with the up-regulation of iron-sulfur cluster assembly and repair functions in biofilm cells. Significant up-regulation of several β-specific glycosidases was also noted in biofilm cells, despite the fact that maltose was the primary carbon source fed to the chemostat. The reasons for increased β-glycosidase levels are unclear but are likely related to the processing of biofilm-based polysaccharides. In addition to revealing insights into the phenotype of sessile *T. maritima* communities, the methodology developed here can be extended to study other anaerobic biofilm formation processes as well as to examine aspects of microbial ecology in hydrothermal environments.**

Mesophilic bacteria in natural and pathogenic environments are often associated with biofilms. This localization facilitates interactions and coexistence in an optimized microenvironment while at the same time limiting the adverse consequences of competition and selectivity (12). The establishment of a sessile community of cells encapsulated by a polysaccharide matrix on a surface involves a complex series of steps: initial attachment, production of exopolysaccharides, early biofilm development, mature biofilm formation, and detachment of cells, perhaps as communities (49, 96). These steps have been investigated for several mesophilic bacteria, including *Pseudomonas aeruginosa* (20, 105), *Bacillus cereus* (71), *Vibrio cholerae* (127), and a *Streptococcus* sp. (100). Biofilm formation apparently requires expression of a distinct set of genes that differentiate sessile from planktonic cells, including those related to chemotaxis, motility, exopolysaccharide biosynthesis, and stress response (88). However, this set of genes may only comprise about 1% of the total genome such that differences between planktonic and sessile cells may be subtle (28, 121). This is not surprising, since biofilm-bound populations likely include newly recruited cells that have a planktonic phenotype as well as cells that represent various stages of biofilm formation (90, 119). Furthermore, even interactions between planktonic cells and surfaces can affect gene expression. For *B. cereus*, planktonic cells grown in the presence of biofilm substratum (glass wool) shared common differentially expressed genes with biofilm-bound cells (71). Thus, composite planktonic and sessile communities likely contain a continuous distribution of distinct phenotypes that have temporal and spatial signatures (96).

The capacity to form biofilms is not limited to aerobic, mesophilic bacteria. Biofilms are also evident in high-temperature environments, such as terrestrial geothermal settings and hydrothermal vents (83). Several anaerobic hyperthermophiles (microorganisms with optimal growth temperatures at or above 80°C) have been shown to produce exopolysaccharides (3, 31, 67). These exopolysaccharides form the basis for biofilms, which have been observed in pure cultures of *Archaeoglobus fulgidus* (52), *Thermotoga maritima* (84), and *Thermococcus litoralis* (87), as well as in cocultures of *T. maritima* and *Methanococcus jannaschii* (63, 84). Biofilm formation was induced by elevated pH, decreased and increased growth temperature, high salt, and exposure to UV light, oxygen, or antibiotic in *A. fulgidus* (52) and by ammonium chloride in *T. litoralis* (87).

A key challenge that must be addressed to further explore biofilm formation processes in hyperthermophilic anaerobes is the experimental complexity associated with the growth of these organisms. This problem was addressed with a high-temperature, anaerobic chemostat that was used to generate

* Corresponding author. Mailing address: Department of Chemical Engineering, North Carolina State University, Raleigh, NC 27695-7905. Phone: (919) 515-6396. Fax: (919) 515-3465. E-mail: rmkelly@eos.ncsu.edu.

† Present address: Roswell Park Cancer Institute, Department of Pharmacology and Therapeutic, Buffalo, NY 14263.

‡ Present address: Genencor International, Inc., Palo Alto, CA 94304.

biofilms in cultures of *T. maritima* that could be sampled and examined for differential gene expression patterns by whole-genome cDNA microarrays comparing planktonic to sessile cells. Transcriptional patterns related to the biofilm phenotype in this hyperthermophilic microorganism were then determined and compared to biofilm formation in less thermophilic microorganisms. Such information concerning biofilm formation mechanisms in hyperthermophiles is needed to develop a better understanding of the microbial ecology in hydrothermal habitats, particularly in regard to surface colonization.

MATERIALS AND METHODS

Microorganism and growth conditions. *T. maritima* (DSM 3109) was grown anaerobically on sea salts medium (SSM) containing 40-g/liter sea salts (Sigma Chemical, St. Louis, Mo.), 1-g/liter yeast extract (Fisher Scientific, Pittsburgh, Pa.), 3.1-g/liter PIPES [piperazine-*N*,*N*′-bis(2-ethanesulfonic acid)] buffer (Sigma), 2-g/liter tryptone, 2-ml/liter 0.05% resazurin, and 10-ml/liter 10× Wolin minerals (117). Growth medium was adjusted to pH 6.8 with KOH (Fisher Scientific) and autoclaved prior to use. Batch cultures (50 ml) were inoculated under N_2 (high-purity nitrogen; National Welders, Raleigh, N.C.) headspace, as previously described (77, 85), and were grown at 80°C for 8 to 10 h in oil baths. Maltose (Sigma Chemical, St. Louis) was added to SSM (final concentration, 5 g/liter) as a carbon source prior to inoculation. Continuous cultivation of *T. maritima* was performed in a 2-liter five-neck, round-bottom flask, as previously described (77, 85). A 50-ml batch culture was used to inoculate 1 liter of SSM supplemented with 5-g/liter maltose in the flask. This seed culture was grown at 80°C for 8.5 h under continuous nitrogen sparging, after which medium was fed at a dilution rate of 0.25 h^{-1}. Medium for continuous cultivation was prepared in 9-liter batches at a 1.2× concentration as mentioned above, to which 1 liter of a filter-sterilized maltose solution (50 g) was added immediately after autoclaving. The pH of the culture was continuously monitored with a Chemcadet pH controller (Cole Parmer, Vernon Hills, Ill.) and adjusted by the addition of 1 M NaOH. Temperature was controlled with a Digi-Sense controller (Cole-Parmer, Vernon Hills, Ill.) such that variations were typically ±0.8°C and verified by a mercury glass thermometer inserted into the culture. Steady-state conditions were monitored by following cell counts (see below) and optical densities at 600 nm. All planktonic cell samples were collected from the outlet line into sterile pyrex bottles (see below), from which 1 ml of cells was fixed in glutaraldehyde for cell counting.

Biofilm substrata and collection. Nylon mesh (Sefar America, Hamden, Conn.) and polycarbonate filters (Poretics 0.22-μm pore diameter; Fisher Scientific, Pittsburgh, Pa.) were used as substrata for biofilm formation. Twelve squares of mesh (13.3 by 9.8 cm) were cut, rolled tightly, and tied with polycarbonate string. Three rolled mesh squares were tied to one another at the ends. Polycarbonate filters were tied to the center of each set of mesh squares to be used for biofilm imaging, while the mesh itself provided biomass for RNA samples within the biofilm. The mesh and loose polycarbonate filters were placed in the reactor and autoclaved prior to startup. The strings were suspended in the growing culture until the sample was collected, whereby they were pulled quickly through one of the five necks of the reactor. The mesh samples and polycarbonate filters were rinsed twice in sterile medium while on ice to remove loosely adhered planktonic cells. Polycarbonate filters were removed from each tube and placed in 2.5% glutaraldehyde (Sigma) to fix the biofilm cells for examination and imaging under the microscope (see below). The mesh squares were separated from the strings and submerged in 50-ml conical tubes containing 300 mM NaCl (Fisher Scientific). The conical tubes were vortexed vigorously (4°C) to remove biofilm material from the mesh, after which the mesh was removed and the resulting suspension was centrifuged (10,000 × *g*, 20 min, 4°C) to pellet the biofilm cell material. Rinse media and 300 mM NaCl were chilled at 4°C prior to use. RNA was extracted as described below.

Imaging and microscopy methods. Epifluorescent micrographs were taken with a SPOT digital camera (Southern Micro Instruments, Atlanta, Ga.) attached to a Nikon (Labophot-2) microscope (Southern Micro Instruments) with 100× oil immersion lens. Planktonic cell suspensions were fixed in 2.5% glutaraldehyde and stained with acridine orange (1 g/liter; Fisher Scientific) to determine cell densities (77, 85). Biofilm cells on polycarbonate filters were fixed as described above, stained in acridine orange (1 g/liter), and dried briefly under vacuum prior to imaging. A scanning electron microscope (JEOL JSM-35CF Microscope, North Carolina State University, Department of Veterinary Medicine) was also used to image biofilm cells on polycarbonate filters. Filters were fixed in 2.5% glutaraldehyde and critically point dried in CO_2. Images of reactor walls of the continuous culture were also taken regularly with a Nikon Coolpix 950 digital camera.

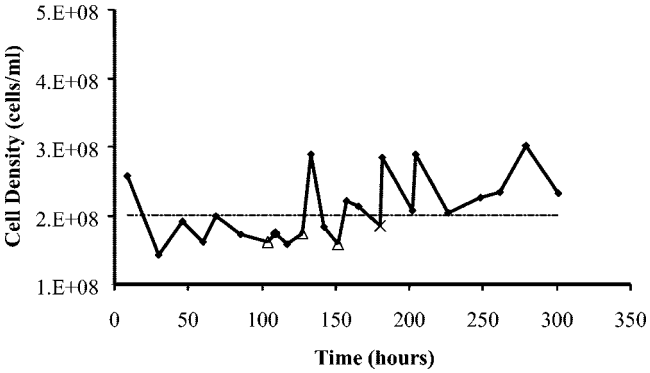

FIG. 1. *T. maritima* growth in 1.5-liter continuous culture at 80°C. Planktonic samples were collected at points designated by △, and biofilm samples were collected at the time noted by ×.

RNA sample collection. Approximately 200-ml samples of planktonic cells were withdrawn through culture outlet (77) into sterile Pyrex bottles on ice. Fifty milliliters of cells was collected prior to sampling to eliminate existing fluid in the lines. The 200-ml samples were used for RNA extractions and processed as described previously (14). Biofilm pellets were rinsed once after being extracted in 300 mM NaCl (4°C) and used immediately for RNA isolation (i.e., RNase-inhibiting buffers were added directly after rinsing step). Total RNA from planktonic cells was extracted from samples from three different time points (Fig. 1) during the steady-state operation; approximately 1 mg of RNA was obtained from each sampling time from which 100 μg was pooled. Similarly, total RNA from the three rolls of mesh from one point in the middle of the chemostat run was pooled to produce a biofilm sample. The cDNA generated from the planktonic and biofilm cells was hybridized to glass slides containing the targeted microarray, scanned, and analyzed, as described previously (15).

Construction of the whole-genome cDNA microarray. Open reading frames (ORFs) were identified from the *T. maritima* MSB8 genome available at http://www.tigr.org/tigrscripts/CMR2/GenomePage3.spl?database = btm. DNA primers were designed with similar annealing temperatures and minimal hairpin formation with Genomax (Informax, Bethesda, Md.). Probes were PCR amplified in a PTC-100 Thermocycler (MJ Research, Inc., Waltham, Mass.) using *Taq* polymerase (Boehringer, Indianapolis, Ind.) and *T. maritima* genomic DNA, isolated as described previously (14). Purification of PCR products and microarray construction were performed by protocols described elsewhere (14). PCR products were randomized within plates before printing with a random number generator, and each gene was applied as a spot six times on each array.

Labeling and hybridization. The whole-genome microarray was interrogated by methods previously described (14). Briefly, first-strand cDNA was prepared from *T. maritima* total RNA using Stratascript (Stratagene, La Jolla, Calif.) and random hexamer primers (Invitrogen Life Technologies, Carlsbad, Calif.); 5-[3-Aminoallyl]-2′-deoxyuridine-5′-triphosphate (Sigma) was used for dye incorporation, as described elsewhere (34). Each biofilm or planktonic cDNA sample was labeled with Cyanine-3 and Cyanine-5, and the samples hybridized to different arrays. The slides were scanned and processed with a Perkin-Elmer Scanarray Express Lite.

Statistical analyses and determination of differential gene expression. Replication of treatments, arrays, dyes, and cDNA spots allowed the use of analysis of variance (ANOVA) models for data analysis (122). Cyanine-3-labeled biofilm cDNA and Cyanine-5-labeled planktonic cDNA were hybridized on one chip, and Cyanine-3-labeled planktonic cDNA and Cyanine-5-labeled biofilm cDNA were hybridized on another chip. The data import code and statistical analysis procedures reported previously (14) were used to analyze spot intensities obtained from Quantarray. Briefly, a linear normalization ANOVA model (122) was used to estimate global variation in the form of fixed (dye, D; treatment, T) and random [array, A; spot, $A(BS)$; block, $A(B)$] effects and random error using the model $\log_2(y_{ijklmn}) = \mu + A_i + D_j + T_k + A_i(B_l) + A_i(S_m \cdot B_l) + \varepsilon_{ijklm}$. A gene-specific ANOVA model was then used to partition the remaining variation into gene-specific effects using the model $r_{ijklm} = \mu + A_i + D_j + T_k + A_i(B_l) + A_i(S_m \cdot B_l) + \varepsilon_{ijklm}$. Volcano plots were used to visualize interesting contrasts or comparisons between two treatments (122). A statistical test with the null

hypothesis of no differential expression was performed for each of the 1,880 ORFs included on the array. A Bonferroni correction was used to adjust α for the expected increase in false positives due to multiple tests (122). The Bonferroni correction, calculated by dividing 0.05 by 1,880, yielded a corrected α of 0.00003, equivalent to a $-\log_{10}$ (*P* value) of 4.5. Genes meeting this significance criterion and showing fold changes of ±2.0 or greater were selected for further examination.

For complete information on significance of expression changes and fold changes, see our website (to be included on our microarray data page at http://www.che.ncsu.edu/extremophiles/microarray/).

RT-PCR confirmation of gene expression. Real-time reverse trasnscription-PCR (RT-PCR) was used to confirm the microarray results of four up-regulated genes (TM0851, 2.3-fold; TM1645, 8.1-fold; TM1848, 6.9-fold; TM1867, 5.1-fold) and one unchanged, control gene (TM0403, 1.2-fold). Primers were designed with Genomax software: TM0851 (GCATAACCGTCAGGATAGGAAG and TTCGACGTGAAGAGGTACACAC), TM1645 (TGTCATGCTGGACAATC TCTCT and ACTTCCACGATCACGTTAGGAT), TM1848 (ATGGAAGCAC TTACCACCAGTT and CCAGTCACCTGTCTCTTTGATG), TM1867 (GGA GAACATGGAGATTCAGAGG and ATCGCACTTCTGACAAATCTGA), and TM0403 (AGGTGATGCTTCTCATAGCGGT and ATCCTAATGCAAT CCAGCAGATCCA). RT of RNA to cDNA was performed as described above. RT-PCR was performed with the SYBRGREEN kit and iCycler iQ real-time PCR detection system (Bio-Rad Laboratories, Hercules, Calif.) according to the manufacturer's protocols. Briefly, reactions for 10 ng of samples were carried out for the five genes at three different temperatures to determine the optimum S-curves. Optimization indicated that all reactions could be performed at 55°C. Standard curves (20, 4, 0.8, and 0.16 ng) for biofilm samples were run along with 10 ng of planktonic and biofilm samples for each gene. Quantitative results were calculated with vendor-provided software (Bio-Rad Laboratories). In all cases, RT-PCR results exhibited the same patterns as those obtained from cDNA microarray analysis. Fold changes calculated from real time PCR were as follows: TM0851, 6.7-fold; TM1645, 10.0-fold; TM1867, 51.1-fold; TM1848, 17.4-fold; and TM0403, 1.3-fold. In all cases of differentially expressed genes, the microarray tended to underestimate the fold changes calculated by real-time PCR, which is not surprising given the smaller dynamic range of microarray scanners when compared to real time PCR.

RESULTS AND DISCUSSION

***T. maritima* growth in continuous culture and biofilm formation.** Because efforts with batch culture were unsuccessful in generating sufficient attached cellular material for transcriptional analysis, a high-temperature anaerobic chemostat was operated to collect *T. maritima* biofilm formed on removable nylon mesh. The mesh was used to create a compact, high-surface-area substratum for biofilm attachment; materials like this have been used successfully to study *P. aeruginosa* biofilms (19). *T. maritima* (T_{opt} 80°C) (37) was grown in continuous culture (dilution rate, $D = 0.25\ h^{-1}$) for over 300 h (Fig. 1). Figure 2A shows the formation of substantial wall growth in the 80°C reactor (86). Epifluorescent micrographs of polycarbonate filters placed in the chemostat showed significant cell attachment at 80°C (Fig. 2B); this was supported by scanning electron microscopy (SEM) analysis of biofilm cells on the filters which showed cells associated with rope-like structures, consistent with SEM analysis of mesophilic biofilms (Fig. 2C) (22, 24, 40).

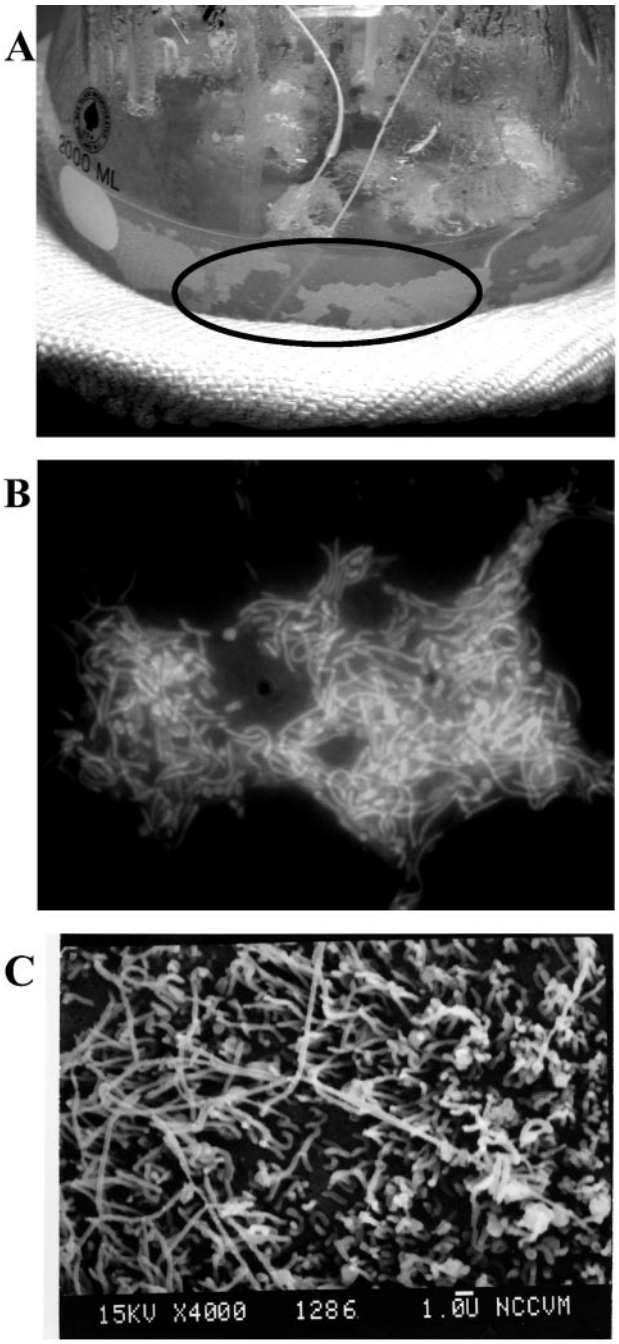

FIG. 2. *T. maritima* biofilm formation on (A) nylon mesh and reactor walls during continuous cultivation. Polycarbonate filters inserted into the culture showed microcolony formation by (B) epifluorescent microscopy and (C) scanning electron microscopy.

Whole-genome cDNA microarray analysis of differential gene expression of sessile and planktonic *T. maritima*. Despite the inherent heterogeneity of the biofilm state, planktonic and sessile *T. maritima* cells could be differentiated by transcriptional response patterns as determined by cDNA microarray analysis (Fig. 3). Table 1 lists genes exhibiting significant expression changes (twofold or higher, $-\log_{10} P$ value of ≥4.5) for biofilm cells as compared to planktonic cells. The cDNA microarray results were confirmed by real-time RT-PCR (see Materials and Methods). For *T. maritima*, approximately 114 genes of the entire genome were differentially expressed twofold or higher at this significance level; 43 of these 114 genes were originally annotated as hypothetical proteins (65). *T. maritima* gene expression patterns were further analyzed according to function, genomic location, and in comparison to biofilm gene expression profiles in mesophilic bacteria. A complete list of expression changes for predicted operons responding signif-

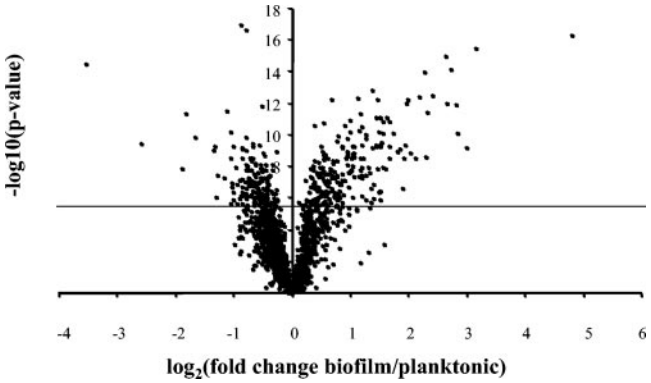

FIG. 3. Volcano plot showing differential gene expression in planktonic and biofilm *T. maritima* cells grown in chemostat culture at 80°C. A horizontal line indicates Bonferroni correction.

icantly between biofilm and planktonic cells is shown in Table 2. Where appropriate, gene annotations are updated with information from comparative genomics and functional studies subsequent to the publication of the *T. maritima* genome sequence (65).

Oxidative and thermal stress response. Biofilm formation has been observed as a response to oxidative stress in the hyperthermophilic archaeon *A. fulgidus* (52), and certain aerobic mesophilic biofilms showed increased expression of oxidative stress genes (29, 91). Increased protein levels of superoxide dismutase and alkyl hydroperoxide reductase in aerobic mesophile biofilms have also been reported (90). Here, the observed down-regulation of predicted operon members rubrerythin (TM0657, −3.7-fold), superoxide reductase (SOR, TM0658, −3.4-fold), and rubredoxin (TM0659, −3.1-fold) in biofilm cells, along with an *ahpC*-related alkylhydroperoxide reductase (TM0807, −6.0-fold), was somewhat unexpected. All four proteins share high identity (57 to 67%) to homologs in *Pyrococcus* species (9, 16, 38, 44). The *Pyrococcus* homologs of rubredoxin and SOR are known to be involved in the NADPH-dependent detoxification of dioxygen to H_2O_2 (38), while a *Pyrococcus horikoshii* AhpC homolog (69% identity, 214 amino acids [aa] with TM0807) participates in a pathway responsible for the reduction of H_2O_2 to alcohol (44). However, an AhpC-related gene (TM0780) encoding a putative thioredoxin peroxidase/bacterioferritin comigratory protein (Bcp) was up-regulated 2.6-fold in biofilm cells (39). A second related gene (TM0386, 3.0-fold), containing an apparently unique combination of a Bcp thioredoxin peroxidase domain and a nitroreductase domain, was also up-regulated.

Several possible explanations exist for the down-regulation of the SOR gene cluster. Lower expression of these genes has been observed during the stationary phase (M. R. Johnson and R. M. Kelly, unpublished data); therefore, decreases in expression here may reflect similarities between stationary-phase and biofilm cells. Alternatively, down-regulation of these genes may suggest lower residual oxygen exposure for cells trapped within a biofilm matrix, although both *T. maritima* planktonic and biofilm cells were cultured in the same anaerobic chemostat. Finally, the down-regulation may reduce exposure of biofilm cells to hydrogen peroxide during oxygen detoxification. Work in *E. coli* K-12 has implicated cysteine as the reductant responsible for rapid recycling of iron(II) to iron(III), allowing reactions between hydrogen peroxide and iron(III) to drive the formation of DNA-damaging hydroxyl radicals (75). Indications of DNA damage in *T. maritima* biofilm cells were observed in the up-regulation of genes encoding a homolog of Sms/RadA (TM0199, 4.6-fold) involved in recombination and repair in *E. coli* K-12 (6), a putative endonuclease specific to archaea (TM0664, 2.3-fold), and a predicted endonuclease (TM1545, 2.0-fold) related to proteins involved in recombination events. DNA protection and repair proteins were also induced in *Listeria monocytogenes* biofilms (107).

Gene expression analysis of biofilm-bound *T. maritima* cells revealed the induction of genes implicated in thermal stress response. Here, biofilm cells displayed 2.3-fold-higher expression of the CIRCE (controlling inverted repeat of chaperone expression)-binding HrcA repressor (TM0851), which controls expression of major heat shock operons in a number of species. We have previously noted the conservation of the CIRCE element upstream of the *T. maritima hrcA-dnaJ-grpE* and *groESL* operons (TM0849 to TM0851) but not upstream of *dnaK-smHSP* (TM0373 to TM0374) (78). Thermal stress genes have been shown to be up-regulated in biofilms of *P. aeruginosa* (*groES* and *dnaK*) (121) and *S. mutans* (*grpE* and *dnaK*) (100). *T. maritima grpE* (TM0850, 1.7-fold), *dnaJ* (TM0849, 1.4-fold), *dnaK* (TM0373, 1.9-fold), heat shock protein class I gene (TM0374, 2.3-fold), and *groES* (TM0373, 1.4-fold) were all up-regulated in biofilm cells. It was interesting that a cold shock protein (TM1874, −2.8 fold) recently shown to act as a functional homolog of product of the RNA-binding *E. coli* K-12 *cspA* gene was down-regulated (76). Schembri et al. (91) also observed down-regulation of the cold shock protein encoded by *cspA* in a microarray experiment comparing *E. coli* K-12 biofilm and exponential-phase planktonic cells.

Exopolysaccharide biosynthesis and degradation. A 2.0-fold upregulation of TM1535 (octaprenyl pyrophosphate synthase) involved in isoprenoid chain synthesis was observed in biofilm cells. Isoprenoid chains serve as scaffolds or lipid carriers for the assembly of monosaccharides into linear and/or branched polysaccharide chains via glycosyl transferases (112). Despite the presence in the *T. maritima* genome of a large cluster of glycosyltransferases, very few were differentially regulated between biofilm and planktonic cells. In fact, a number were expressed 1.5- to 1.7-fold higher in planktonic cells, including TM0630, an NDP-sugar epimerase related to UDP-glucose-4-epimerases; TM0627, a putative NDP-linked sugar glycosyltransferase; and TM0818, a techoic acid biosynthesis protein related to GumM in *Xanthomonas campestris* pv. *gum* (data not shown). A glycosyltransferase (TM0392, −2.2) predicted to be involved in the synthesis of NDP-linked sugars was also down-regulated in biofilm cells, while a homolog of *E. coli* K-12 *ushA* which encodes a periplasmic protein with UDP-sugar hydrolase activity (11) was up-regulated (TM1878, 2.3 fold). It is possible that exopolysaccharide synthesis occurs both in biofilm and planktonic cells, since commonalities in expression patterns have been observed between biofilm cells and planktonic cells in the presence of biofilm substratum (71).

Glycosyl hydrolases may also be involved in exopolysaccharide synthesis and/or degradation. Induction of an NAD^+-dependent family 4 α-glucuronidase (TM0752, 3.1-fold) (99) and a β-galactosidase (TM0310, 2.9-fold) was observed in the

TABLE 1. *T. maritima* ORFs differentially regulated in biofilm[a]

Gene description	Source of gene description (reference)	Gene ID	Fold change	$-\text{Log}_{10}$ *P* value
Upregulated in biofilm[b]				
Aspartate dehydrogenase	(124)	TM1643	27.9	16.3
ThiH protein, putative	28% identity, 347 aa with *E. coli* ThiH (53, 104) conserved CX_3CX_2C [4Fe-4S] cluster binding motif	TM1267	8.9	15.4
Nicotinate-nucleotide pyrophosphorylase (NadC)	Crystallized (GI:34811257; 1O4U_A, 1O4U_B)	TM1645	8.1	9.1
Hypothetical protein	(65)	TM1266	7.2	10.0
Quinolinate synthetase A (NadA)	54% identity, 298 aa with *P. abyssi* (PAB2345) and *P. horikoshii* (PH0013), 3 conserved cysteines	TM1644	7.1	11.9
Cellobiose phosphorylase	(79)	TM1848	6.9	12.9
Cation-transporting ATPase, P-type	COG2217, 30% identity, 724 aa with *E. coli* ZntA (93)	TM0317	6.6	14.1
SufD homolog, similar to ABC permease components	COG0719	TM1370	6.3	12.0
SufB homolog, similar to ABC ATP-binding components	(80)	TM1369	6.3	15.0
Iron(II) transport protein B (FeoB)	33% identity, 718 aa with *E. coli* FeoB (43, 60)	TM0051	5.4	12.4
L-Lactate dehydrogenase	(72)	TM1867	5.1	11.0
Ubiquinone/menaquinone methyltransferase	COG0500, SAM-dependent methyltransferases, 53% identity, 452 aa with PF0738	TM0318	5.0	11.4
Biotin synthetase, putative (BioB homolog)	22% identity, 281 aa with *E. coli* BioB (108) conserved CX_3CX_2C motif, CX_2C motif	TM1269	5.0	8.6
IscS/SufS homolog, cysteine desulfurase	(59)	TM1371	4.8	13.9
Sms/RadA homolog, DNA recombination/repair protein	39% identity, 452 aa with *E. coli* Sms/RadA (6), conserved $CX_2CX_{10}CX_2C$ motif is a zinc finger in *E. coli* Sms/RadA	TM0199	4.6	12.4
FTR1, predicted high-affinity Fe^{2+}/Pb^{2+} permease	25% identity 228 aa with *S. cerevisiae* Ftr1p; two conserved REXXE iron-binding motifs (95)	TM0417	4.4	8.5
Esterase, putative	(65)	TM0053	4.1	8.8
Iron(II) transport protein A (FeoA)	42% identity 57 aa with *E. coli* FeoA (43)	TM0050	4.0	12.2
Cysteine synthase (CysK)	Crystal structure (GI:34810052, IO58A-IO8D)	TM0665	3.9	12.0
Serine acetyltransferase (CysE)	43% identity, 195 aa with *S. xylosus* CysE (26)	TM0666	3.9	9.3
FpaA family protein, contains flavodoxin domain and β-metallo-lactamase domain	COG0426, 28% identity, 366 aa with *D. gigas* ROO (27)	TM0755	3.8	8.5
Hypothetical protein	(65), 32% identity, 78 aa with TTE1569	TM1268	3.7	6.6
Uncharacterized homolog of γ-carboxymuconolactone decarboxylase	COG0599	TM0316	3.6	9.1
NADH oxidase	46% identity, 440 aa with *T. neapolitana* NADH: polysulfide oxidoreductase	TM0395	3.5	9.0
Ubiquinone/menaquinone biosynthesis methyltransferase, putative (UbiE homolog)	COG2226	TM0753	3.3	10.1
HycB domain containing protein, related to hydrogenase components	COG1142, 2 $CX_2CX_2CX_3C$ motifs, 1 $CX_2CX_7CX_2C$ motif, 1 $CX_2CX_4CX_3C$ motif	TM0396	3.2	10.8
Heavy metal binding protein	(65)	TM0320	3.2	9.2
Uncharacterized conserved protein	COG3862, CX_2CX_3C motif	TM1434	3.2	8.5
Predicted zinc-dependent protease	COG2738	TM1511	3.1	11.0
NAD^+-dependent α-glucuronidase	(99)	TM0752	3.1	7.9
Protein containing Bcp domain and nitroreductase domain	COG1225 (Bcp domain), COG0778 (nitroreductase domain)	TM0386	3.0	3.1
Hypothetical protein	(65)	TM0338	3.0	7.9
Hypothetical protein	(65)	TM0052	3.0	10.1
Predicted GTPase	COG1160	TM0445	2.9	10.8
β-D-Galactosidase	40% identity, 670 aa with *B. stearothermophilus* β-galactosidase (36)	TM0310	2.9	9.5
IscU/SufA homolog, iron-sulfur cluster assembly scaffold	3 conserved cysteines bind a [2Fe-2S] cluster (8, 58)	TM1372	2.9	5.9
Uncharacterized conserved protein	COG0011, pfam01910, localized with TauABC (4 species)	TM0486	2.9	9.4
ABC transporter, permease protein, TauC family	COG0600	TM0485	2.9	11.1
ATP-dependent Clp protease, ATPase subunit, ClpA homolog	COG0542	TM0198	2.8	9.2
Glutamate synthase domain 3 (GltB)	COG0070	TM0394	2.8	6.5
Possible endonuclease or sugar phosphate isomerase	COG1082, pfam01261	TM0422	2.8	6.3

Continued on facing page

TABLE 1—*Continued*

Gene description	Source of gene description (reference)	Gene ID	Fold change	$-\text{Log}_{10}$ *P* value
Hypothetical protein	(65)	TM0054	2.8	10.2
Predicted membrane protein	COG3462	TM0315	2.8	12.2
Uncharacterized conserved protein	COG0718	TM0687	2.8	7.9
Cystathionine γ-synthase/β-lyase	COG0626	TM1270	2.7	9.3
Predicted transcriptional regulator, ACR/TetR related	pfam00440	TM0823	2.7	9.2
Sugar ABC transporter, permease protein, UpgA family	COG1175	TM0419	2.7	11.0
Sugar ABC transporter, periplasmic sugar-binding protein, MalE-related	COG2182	TM0418	2.7	6.9
ABC transporter, ATP-binding subunit, TauA family	COG0715	TM0484	2.6	5.9
Hypothetical protein	(65)	TM0714	2.6	9.2
Thioredoxin peroxidase	COG1225, 59% identity, 157 aa with *T. acidophilum* (Tal1368M)	TM0780	2.6	12.8
Hypothetical protein	(65)	TM0319	2.6	6.6
Predicted HHH nucleic acid binding protein	COG1623, pfam02457	TM0200	2.6	5.7
Glycerol uptake facilitator protein	COG0580	TM1429	2.5	7.6
FixX homolog, putative ferredoxin	COG2440, $CX_3CX_4CX_3CC$ motif, $CX_2CX_2CX_3C$ motif	TM1533	2.5	5.3
FixC homolog	42% identity, 438 aa with *A. caulinodans* FixC (4)	TM1532	2.5	7.9
PotD, spermidine/putrescine ABC transporter, PBP	39% identity, 320 aa with *E. coli potD* (45)	TM1375	2.5	2.6
Transcriptional regulator, biotin repressor family	Crystallized (GI:22218828, 1J5YA)	TM1602	2.4	9.7
Predicted CAAX amino-terminal protease	pfam0257	TM1529	2.4	10.0
RAD55-related, RecA superfamily ATPase	COG0467, 78% identity, 235 aa with PH0824, PAB2180, PH1931	TM0370	2.4	7.4
Pyridine nucleotide-disulfide oxidoreductase, putative	pfam00070	TM0754	2.4	5.9
Oxidoreductase, aldo/keto reductase family	COG0467	TM1743	2.4	7.2
NADH:polysulfide oxidoreductase	86% identity, 440 aa with *T. neapolitana* (GI:21702687)	TM0379	2.3	8.5
Hypothetical protein	(65)	TM0002	2.3	9.4
Heat shock operon repressor HrcA	(65, 78)	TM0851	2.3	7.3
Conserved hypothetical protein, GGDEF domain	COG2199, pfam00990	TM1588	2.3	7.5
Glutamate synthase domain 2, GltB	COG0069, pfam01645, CX_2CX_2C motif	TM0397	2.3	7.9
UDP-sugar disphosphatase precursor	38% identity, 504 aa with *E. coli* UshA (11)	TM1878	2.3	7.9
Putative endonuclease	COG1833, pfam01986	TM0664	2.3	10.5
Uncharacterized conserved protein	COG4198, pfam06245	TM1510	2.3	6.1
Membrane bound protein LytR, putative transcriptional regulator	COG1316, pfam03816	TM1866	2.3	9.8
FixA homolog, electron transfer flavoprotein	45% identity, 241 aa with *A. caulinodans* FixA (4)	TM1530	2.3	1.9
Sugar ABC transporter, ATP-binding protein, MalK homolog	COG3839	TM0421	2.3	11.3
Heat shock protein, class I	(62)	TM0374	2.3	8.5
Conserved hypothetical protein	(65)	TM0387	2.3	7.8
Predicted coenzyme A-binding protein	COG1832	TM1435	2.2	7.3
Conserved hypothetical protein	pfam03706	TM1390	2.2	10.2
Hypothetical protein	(65)	TM1534	2.2	12.3
Frameshift	(65)	TM0621	2.2	5.2
Glutamate synthase domain 1, GltB	COG0067	TM0398	2.2	5.2
Putative sensor histidine kinase	(65)	TM0187	2.2	5.3
Conserved hypothetical protein	pfam01139	TM1357	2.1	8.8
ABC transporter, ATP-binding subunit, SalX domain	COG1136	TM0352	2.1	9.2
Endoglucanase (extracellular)	(15, 57)	TM1525	2.1	8.6
Iron(III) ABC transporter, ATP-binding protein, putative	COG1120, 50% identity, 242 aa with *P. furiosis* (PF0909)	TM0191	2.1	7.3
Putative transcriptional regulator	COG1318, 58% identity, 150 aa with *P. horikoshii* (PH0283)	TM0369	2.1	8.0
Iron-sulfur cluster-binding protein, putative	COG2768, 2 $CX_2CX_2CX_3C$ motifs (65)	TM0034	2.1	6.0
Heat shock serine protease, periplasmic	(46, 47)	TM0571	2.1	9.3
Hypothetical protein	(65)	TM0003	2.0	8.7

Continued on following page

TABLE 1—*Continued*

Gene description	Source of gene description (reference)	Gene ID	Fold change	$-\text{Log}_{10}$ *P* value
Permease, putative	COG0477, 36% identity, 409 aa with *B. subtilis* YceI (50)	TM1603	2.0	7.7
Octaprenyl pyrophosphate synthase	(32, 51)	TM1535	2.0	7.6
Membrane protein, putative	COG3374	TM1536	2.0	8.5
ABC transporter, ATP-binding protein, TauB family	COG1116	TM0483	2.0	10.2
RNA polymerase σ^A factor	(13, 65)	TM1451	2.0	10.9
Putative Holliday junction resolvase	COG0816	TM1545	2.0	10.9
ABC transporter, permease subunit, SalY family	COG0577	TM0351	2.0	8.9
Down-regulated in biofilm[c]				
K^+ channel, beta subunit	COG0667, pfam00248	TM0313	−2.0	9.3
Cyclomaltodextrinase	(54)	TM1835	−2.0	9.6
Putative regulator, XRE family HTH	COG1917, pfam1381	TM0656	−2.0	6.7
Hypothetical protein	(65)	TM0794	−2.1	6.9
Predicted dehydrogenase	COG0673, 67% identity, 325 aa with *P. furiosus* (PF0554)	TM0312	−2.1	5.6
(3*R*)-Hydroxymyristoyl-(acyl carrier protein) dehydratase	COG0764 (65)	TM0801	−2.1	10.1
Uncharacterized conserved protein	COG3906	TM0606	−2.1	8.5
Bacteriocin	33% identity, 251 aa to *B. linens* linocin M18 (109)	TM0785	−2.2	11.4
Maltose ABC transporter, permease protein	(118)	TM1836	−2.2	2.0
Predicted glycosyltransferase	COG0438, pfam00534	TM0392	−2.2	7.3
Hypothetical protein	(65)	TM1241	−2.4	7.4
Uncharacterized conserved protein	COG3471	TM0786	−2.4	6.0
Ribosomal protein L7/L12	(65)	TM0457	−2.5	9.3
Ribosomal protein L10	(65)	TM0456	−2.6	9.0
Cold shock protein	(76, 120)	TM1874	−2.8	9.6
Rubredoxin	68% identity, 51 aa with *P. furiosis* rubredoxin PF1282 (9, 21), 2 conserved CXXC motifs	TM0659	−3.1	9.9
Superoxide reductase (neelaredoxin)	57% identity, 128 aa with *P. furiosis* SOR (PF1281) (38, 125)	TM0658	−3.5	11.4
Rubrerythrin	58% identity, I65 aa with *A. fulgidus* rubrerythrin (AF1640) (115)	TM0657	−3.7	7.8
NADPH-dependent alkyl hydroperoxide reductase	69% identity, 214 aa with *P. horikoshii* (PH1217) (44)	TM0807	−6.0	9.4
Protein distantly related to bacterial ferritins	COG2406, 82% identity, 183 aa with *M. acetivorans* strain CZA (MA2882)	TM0560	−11.6	14.5

[a] Locus description based on conserved domain searches (CDD, NCBI) and similarity to characterized proteins. Species used: *Archaeoglobus fulgidus*, *Azorhizobium caulinodans*, *Brevibacterium linens*, *Bacillus stearothermophilus*, *Bacillus subtilis*, *Desulfovibrio gigas*, *Escherichia coli K-12*, *Methanosarcina acetivorans* strain C2A, *Pyrococcus furiosus*, *Pyrococcus horikoshii*, *Pyrococcus abyssi*, *Thermoplasma acidophilum*, *Thermotoga neapolitana*, *Saccharomyces cerevisiae*, and *Staphylococcus xylosus*. Bcp, bacterioferritin comigratory protein.

[b] Genes up-regulated 2.0-fold or greater in biofilm. Significance based on Bonferroni-corrected significance criterion with $-\log_{10} P$ value of >4.6.

[c] Genes down-regulated 2.0-fold or greater in biofilm. Significance based on Bonferroni-corrected significance criterion with $-\log_{10} P$ value of >4.6.

apparent absence of growth substrates related to these enzymes. Both proteins have been observed to be up-regulated during early stationary phase in *T. maritima-M. jannaschii* coculture experiments when the formation of biofilm material is observed (M. R. Johnson and R. M. Kelly, unpublished). Cellobiose phosphorylase (CepA) (TM1848) (65) exhibited a 6.9-fold expression increase in biofilm cells compared to planktonic cells at 80°C. CepA from *Thermotoga neopolitana* has sole substrate specificity for cellobiose (126), which it converts to D-glucose and glucose-1-phosphate (68). Characterization of the *T. maritima* homolog revealed substrate specificity for cellobiose in the hydrolysis reaction but relaxed synthetic specificity for the reverse reaction, allowing mannose, xylose, glucosamine, 2- and 6-deoxy-D-glucose, and β-D-glucoside to act as glucosyl acceptors for glucose-1-P (79). The strong up-regulation of this gene was unexpected, since maltose (α-1,6) and not cellobiose (β-1,4) was used as the primary carbon source in the growth medium. The up-regulation of the operon (TM1524 to TM1536) containing β-endoglucanases Cel12B (TM1524) and Cel12A (TM1525) (18, 56), previously shown to be up-regulated on carboxymethylcellulose, barley, and konjac glucomannan (14), was also noted. Further work will be necessary to determine whether the induction of glycoside hydrolases in biofilm cells is related to the synthesis or breakdown of exopolysaccharide-based biofilm material or the sloughing of biofilm.

ABC transporters. Several ABC transporter genes were differentially expressed in biofilm cells. Despite the fact that maltose was the primary carbohydrate in the growth medium, genes within a maltose utilization and transport operon (TM1834 to TM1839) were down-regulated in biofilm cells. On the contrary, genes predicted to encode an uncharacterized multiple-sugar transport system (TM0418 to TM0421) downstream of the FTR1-related iron transporter (TM0417) were

TABLE 2. Differential expression of genes in biofilm-bound cells as related to predicted *T. maritima* operons

Putative function	Gene ID	Gene description	Fold change	$-\text{Log}_{10}$ *P* value[c]
Iron transport[b]	TM0050	Iron(II) transport protein A (FeoA)	4.0	12.2
	TM0051	Iron(II) transport protein B (FeoB)	5.4	12.4
	TM0052	Hypothetical protein	3.0	10.1
	TM0053	Esterase, putative	4.1	8.8
	TM0054	Hypothetical protein	2.8	10.2
DNA processing[b]	TM0198	ATP-dependent Clp protease, ATPase subunit, ClpA family	2.8	9.2
	TM0199	Sms/RadA homolog, DNA recombination/repair protein	4.6	12.4
	TM0200	Predicted HHH nucleic acid binding protein	2.6	5.7
	TM0201	NADP-reducing hydrogenase, subunit D, putative	1.5	2.7
	TM0202	TauA homolog	1.7	5.5
Cation transport system[b]	TM0315	Predicted membrane protein	2.8	12.2
	TM0316	Uncharacterized homolog of γ-carboxymuconolactone decarboxylase subunit	3.6	9.1
	TM0317	Cation-transporting ATPase, P-type	6.6	14.1
	TM0318	Ubiquinone/menaquinone methyltransferase	5.0	11.4
	TM0319	Hypothetical protein	2.6	6.6
	TM0320	Heavy metal binding protein	3.2	9.2
ABC transport[a]	TM0351	ABC transporter, permease subunit, SalY family	2.0	8.9
	TM0352	ABC transporter, ATP-binding subunit, SalX domain	2.1	9.2
	TM0353	Predicted membrane fusion protein (COG0845)	1.4	6.4
DNA repair[a]	TM0369	Predicted transcriptional regulator	2.1	8.0
	TM0370	RAD55-related, RecA superfamily ATPase (COG0467)	2.4	7.4
Thermal stress	TM0373	DnaK protein (62)	1.9	8.5
	TM0374	Heat shock protein, class I	2.3	8.5
Glutamate synthesis[a]	TM0394	Glutamate synthase domain 3 (GltB)	2.8	6.5
	TM0395	NADH oxidase	3.5	9.0
	TM0396	HycB domain containing protein, related to hydrogenase components	3.2	10.8
	TM0397	Glutamate synthase domain 2, GltB	2.3	7.9
	TM0398	Glutamate synthase domain 1, GltB	2.2	5.2
Sugar and iron transport[b]	TM0417	FTR1, predicted high affinity Fe^{2+}/Pb^{2+} permease	4.4	8.5
	TM0418	Sugar ABC transporter, periplasmic sugar-binding protein, MalE-related	2.7	6.9
	TM0419	Sugar ABC transporter, permease protein, UpgA family	2.7	11.0
	TM0420	Sugar ABC transporter, permease protein	1.4	7.6
	TM0421	Sugar ABC transporter, ATP-binding protein, MalK homolog	2.3	11.3
	TM0422	Possible endonuclease or sugar phosphate isomerase	2.8	6.3
Sulfur compound transport systems[a]	TM0483	ABC transporter, ATP-binding protein, TauB family	2.0	10.2
	TM0484	ABC transporter, ATP-binding subunit, TauA family	2.6	5.9
	TM0485	ABC transporter, permease protein, TauC family	2.9	11.1
	TM0486	Uncharacterized conserved protein	2.9	9.4
Oxygen detoxification[a]	TM0657	Rubrerythrin	−3.7	7.8
	TM0658	Superoxide reductase (neelaredoxin)	−3.5	11.4
	TM0659	Rubredoxin	−3.1	9.9
Amino acid metabolism[b]	TM0664	Putative endonuclease	2.3	10.5
	TM0665	Cysteine synthase	3.9	12.0
	TM0666	Serine acetyltransferase (CysE)	3.9	9.3
Oxygen detoxification/electron transfer[b]	TM0752	NAD^+-dependent α-glucuronidase	3.1	7.9
	TM0753	Ubiquinone/menaquinone biosynthesis methyltransferase, putative (UbiE homolog)	3.3	10.1
	TM0754	Oxidoreductase	2.4	5.9
	TM0755	FpaA family protein, contains flavodoxin domain and β-metallolactamase domain (COG0426)	3.8	8.5

Continued on following page

TABLE 2—*Continued*

Putative function	Gene ID	Gene description	Fold change	$-\text{Log}_{10}$ *P* value[c]
Biotin/thiamine-synthesis[b]	TM1266	Hypothetical protein	7.2	10.0
	TM1267	ThiH protein, putative	8.9	15.4
	TM1268	Hypothetical protein	3.7	6.6
	TM1269	Biotin synthetase, putative (BioB homolog)	5.0	8.6
	TM1270	Cystathionine γ-synthase/β-lyase	2.7	9.3
Iron-sulfur cluster assembly[a]	TM1368	SufC homolog, similar to ABC ATP-binding components	1.1	2.0
	TM1369	SufB homolog, similar to ABC permease components	6.3	15.0
	TM1370	SufD homolog, similar to ABC permease components	6.3	12.0
	TM1371	SufS/IscS homolog, cysteine desulfurase	4.8	13.9
	TM1372	SufA/IscU homolog, iron-sulfur cluster assembly scaffold	2.9	5.9
Sugar/electron transfer cascade[b]	TM1524	Endoglucanase (intracellular)	1.8	7.1
	TM1525	Endoglucanase (extracellular)	2.1	8.6
	TM1526	Hypothetical protein (COG1633)	1.7	6.3
	TM1527	IscR homolog, putative	1.8	6.0
	TM1528	1,4-Dihydroxy-2-naphthoate octaprenyltransferase, MenA homolog	1.7	6.0
	TM1529	Predicted CAAX amino terminal protease	2.4	10.0
	TM1530	FixA homolog, electron transfer flavoprotein	2.3	1.9
	TM1531	FixB homolog, electron transfer flavoprotein	2.0	4.9
	TM1532	FixC homolog	2.5	7.9
	TM1533	FixX homolog	2.5	5.3
	TM1534	Hypothetical protein	2.2	12.3
	TM1535	Octaprenyl pyrophosphate synthase (OPP)	2.0	7.6
	TM1536	Putative membrane protein	2.0	8.5
Nicotinate synthesis[b]	TM1643	Aspartate dehydrogenase	27.9	16.3
	TM1644	Quinolinate synthetase A (NadA)	7.1	11.9
	TM1645	Nicotinate-nucleotide pyrophosphorylase (NadC)	8.1	9.1
Maltose utilization and transport[b]	TM1834	α-glucosidase	−1.5	5.1
	TM1835	Cyclomaltodextrinase	−2.0	9.6
	TM1836	Maltose ABC transporter, permease protein	−2.2	2.0
	TM1837	Maltose transport system permease protein	−1.9	8.1
	TM1838	Hypothetical protein	−1.4	5.7
	TM1839	Maltose ABC transporter, periplasmic maltose-binding protein	1.0	0.4

[a] Complete operon predicted by www.tigr.org.
[b] Partial operon predicted by www.tigr.org.
[c] Note that some $-\log_{10} P$ values are below the significance criterion Bonferroni factor of 4.6.

up-regulated in biofilm cells along with a gene sharing domain similarity with sugar phosphate isomerases (TM0422, 2.8-fold).

Additional homologs to ABC transporters were up-regulated during biofilm growth (Table 2). It was particularly intriguing to note the up-regulation of two genes which bear similarity to genes encoding antimicrobial peptide exporters. TM0352 (2.1-fold) is predicted to encode an ATP-binding ABC subunit (COG1136), while TM0351 (2.0-fold) possibly encodes an ABC-associated permease component (COG0577). Three additional upstream genes encode a putative membrane fusion protein (TM0353), outer membrane protein (TM0354), and TolC protein (TM0355). These genes (TM0353 to TM0355) were not expressed differentially between biofilm and planktonic conditions. A distantly related, though not well conserved, multiprotein system is essential for biofilm adhesion in *Pseudomonas fluorescens* WCS365, consisting of an ABC ATPase, ABC permease, outer membrane protein, and large adhesion protein with repetitive domains which is secreted via the transporter (35). A glycerol uptake facilitator protein (TM1429) (2.5-fold) was also up-regulated in *T. maritima* biofilm cells; ferric iron and glycerol may be required for antimicrobial peptide release as shown during biofilm growth of bacilli (123).

Response of iron/sulfur uptake and utilization genes in biofilm cells. Biofilm cells showed increased expression of iron and sulfur uptake systems, consistent with up-regulation of genes encoding iron-sulfur cluster-containing proteins and components of a chaperone system involved in iron-sulfur cluster formation and repair. Predicted operons containing these genes are present in a number of distinct regions of the *T. maritima* genome. Known Fe-S clusters or cysteine-rich sequence motifs in the corresponding proteins are noted in Table 2.

Up-regulation of iron uptake is important in mesophile biofilm formation processes (10), which likely relates to the observed induction of genes encoding iron acquisition proteins in

T. maritima biofilm cells. Increased expression was noted for genes encoding homologs of FeoB (TM0051, 5.4-fold), which is a G protein-like iron(II) transport system characterized in several species (2), and FeoA (TM0050, 4.4-fold), also presumed to be involved in iron transport (33). A second putative transporter gene (TM0417, 4.4-fold) related to yeast FTR1 high-affinity Fe^{2+} permeases (95), and the ATP-binding subunit of a putative iron(III) ABC transporter, FepC (TM0191, 2.1-fold), were also induced in biofilm cells. A protein distantly related to bacterial ferritins (TM0560 and COG2406) was the most highly downregulated gene in biofilm cells (−11.6-fold), presumably reflecting a decreased need for iron sequestration (5). Iron uptake regulation mechanisms have not been determined experimentally for *T. maritima*, but a small, statistically significant increase in the expression of a ferric uptake regulator (*fur*) homolog was noted (TM0122, 1.5-fold). Sequences resembling Fur binding sites are found upstream of the predicted iron transporter TM0417 and also upstream of TM0122, which precedes a similarly regulated set of ABC transporter components related to metal uptake systems (data not shown).

Genes (TM0483 to TM0485) homologous to two *E. coli* K-12 ABC transporter systems for sulfonates (25, 111) were preferentially induced in biofilm cells. *E. coli* K-12 and *Rhodobacter capsulatus* (61) *tauABC* encode taurine uptake ABC transporters, while the *ssuABC* operon encodes an alkane sulfonate transport system in *E. coli* K-12 and *B. subtilis* (25, 110). Although the natural substrates of the two *tauABC*-related systems in *T. maritima* have not been determined, sulfates and cysteine are present in the growth medium. Imported taurine and sulfates are typically incorporated via the cysteine biosynthesis pathway, but no recognizable homolog to the *E. coli* TauD desulfonation enzyme is apparent in the *T. maritima* genome. However, homologs to the uncharacterized conserved ORF (TM0486) are found upstream of *tauABC* homologs in two *Streptococcus pneumoniae* strains, *Clostridium acetobutylicum*, and *Corynebacterium glutamicum* (94). Crystal structures of two proteins related to TM0486 (pfam01910) suggest a ferredoxin-like fold and a possible role in protein-protein interaction regulated by the binding of sulfate ions (103). Several genes encoding predicted serine and cysteine biosynthesis enzymes were up-regulated here, including cysteine synthase (TM0665, 3.9-fold), serine acetyltransferase (TM0666, 3.9-fold), and a cystathione β-lyase/cystathione γ-synthase homolog predicted to be involved in cysteine degradation (TM1270, 2.7-fold) (Fig. 4).

The up-regulation of genes encoding members of a predicted iron-sulfur cluster chaperone complex offers insight into the apparent need of biofilm cells to acquire iron and sulfur from the environment and increase synthesis of cysteine. Iron-sulfur cluster synthesis and repair in biofilms may be a more general phenomenon, as a recent report indicates the upregulation of the iron-sulfur chaperones *nifSU* in mature biofilms of *E. coli* K-12 (7). Three paralogous cysteine desulfurases—IscS, NifS, and SufS—have been characterized in *E. coli* K-12 (101). While TM1371 and TM1372 have been referred to as *iscS* and *iscU* in characterization efforts, the lack of other *isc* genes in this genomic region has been noted (8, 58). Recent characterization of the SufABCDES iron-sulfur cluster assembly complex in *E. coli* K-12 (101) suggests a more appropriate designation of *sufS* (TM1371) and *sufA* (TM1372), given the colocalization with *sufBCD* homologs and the known role of SufABCDS in iron-sulfur cluster assembly under conditions of iron limitation and oxidative stress in *E. coli* K-12 (97) and *Erwinia chrysanthemi* (64). A homolog to SufE, which stimulates the cysteine desulfurase activity of SufS in *E. coli* K-12 (70), is not identifiable in *T. maritima*. The proteins encoded by *sufC* (TM1368) and *sufB* (TM1369) have been shown to interact in *T. maritima* cells (80); despite the lack of differential expression of the *sufC* homolog, the distantly related *sufB* and *sufD* (TM1370) are both expressed 6.3-fold higher in biofilm. Structural characterization of SufS/IscS (TM1371) has revealed conformational flexibility consistent with a role in iron-sulfur cluster donation to a variety of proteins, while SufA (TM1372) may act as a scaffold for iron-sulfur cluster assembly (59). A second SufS/IscS homolog in *T. maritima*, previously designated NifS (TM1692) (41), was not differentially expressed here.

Two putative regulators found in the *T. maritima* genome (TM0567 and TM1527) bear sequence similarity to IscR, a negative regulator of the Isc "housekeeping" iron-sulfur cluster assembly complex in *E. coli* K-12 (92). Three cysteine residues in *E. coli* IscR coordinate a [2Fe-2S] cluster which, when destabilized, disrupts DNA binding to IscR and allows transcription of the Isc operon (92). All three conserved cysteine residues are present in TM1527, located within a biofilm up-regulated gene string encoding FixABCX homologs and a hypothetical protein (TM1534, 2.2-fold) with a conserved $CXXCX_{12}CXXC$ motif. While the FixABCX proteins of *T. maritima* have not yet been characterized, homologous proteins function in electron transfer chains in other bacteria, including *Rhizobium meliloti* (23), *Rhizobium leguminosarum* (30), *Azorhizobium caulinodans* (42), and *E. coli* K-12 (116).

Additional plausible targets for Fe-S cluster assembly complexes are suggested by differential expression data. TM0034 (2.1-fold) contains two cysteine-rich sequence motifs, which are predicted to bind iron-sulfur clusters (Fig. 4). Up-regulated genes in a glutamate synthesis operon (TM0394 to TM0398) encode a putative NADH oxidase (TM0395) and three domains of glutamate synthase, a multiple iron-sulfur cluster binding complex (82). Also up-regulated is an iron-sulfur cluster binding protein (TM0396, 3.2-fold) that shares identity (44% identity, 143 amino acids) with a carbon monoxide dehydrogenase from *A. fulgidus*. O'Toole and Kolter (73) have shown that glutamate- and/or iron-containing medium can restore the ability of some biofilm-defective *P. fluorescens* strains to form biofilm.

Two separate predicted operons encoding a number of cofactor biosynthesis enzymes (TM1266 to TM1270 and TM0787 to TM0789) were overexpressed in *T. maritima* biofilm cells. Expression changes for the putative *thi1-thiC* homologs (TM0787 and TM0788), which are most closely related to archaeal thiamine biosynthesis enzymes, but largely absent from other eubacteria, were considerably lower (<2.0-fold) than those of *thiH-bioB-metC* (TM1267, TM1269, and TM1270). *E. coli* K-12 *iscS* mutants have been shown to be deficient in thiamine biosynthesis (53), likely as a result of degradation of an iron-sulfur cluster in the ThiH protein (56). *E. coli* K-12 ThiH is involved in biosynthesis of the thiamine thiazole ring, a process which requires sulfur donation from cysteine to ThiS via IscS (53, 104). The iron-sulfur cluster

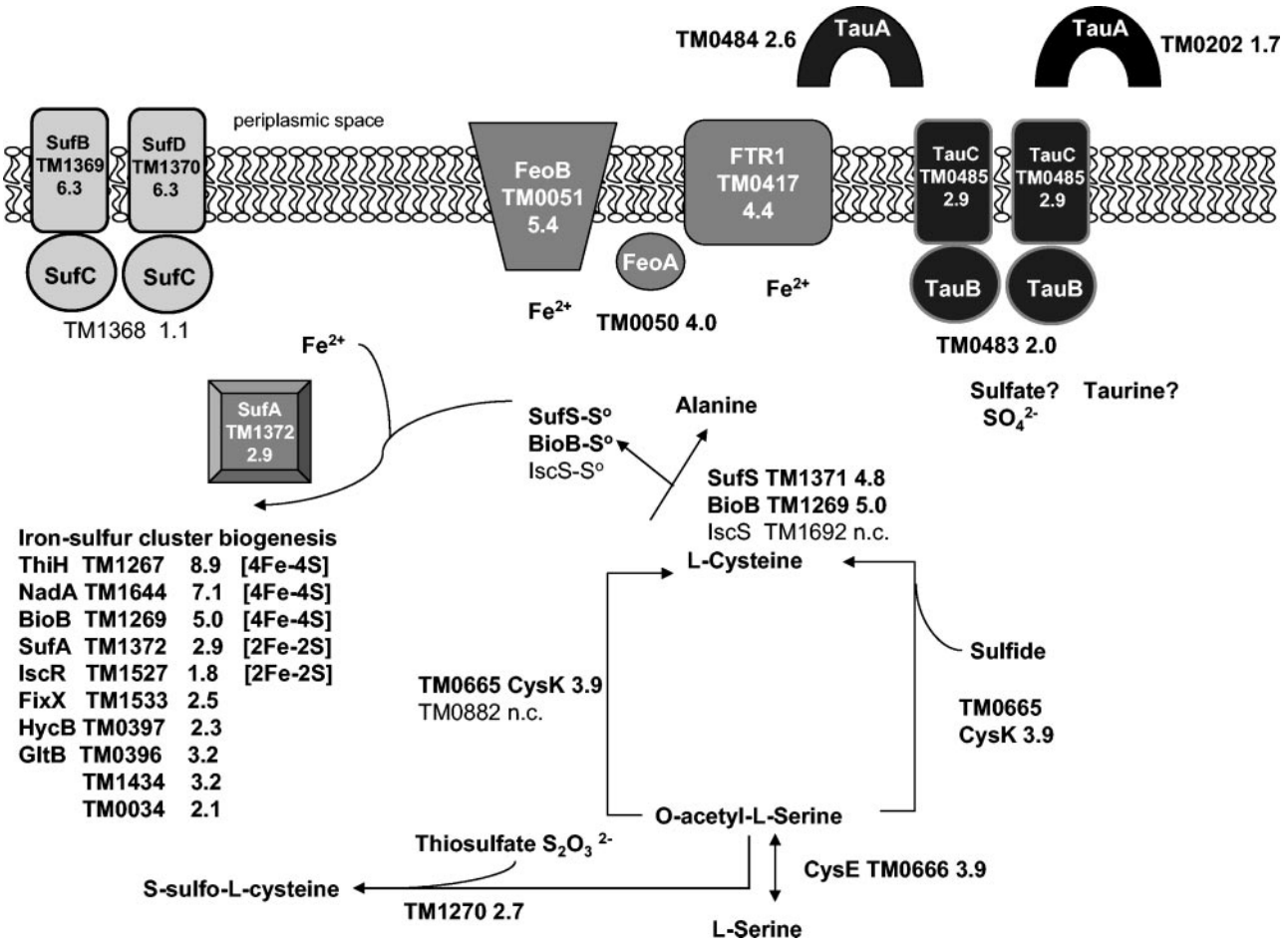

FIG. 4. Predicted pathway for iron-sulfur cluster biogenesis in *T. maritima* biofilm cells. Expression data suggest a number of known iron-sulfur cluster binding proteins and proteins with conserved cysteine-rich motifs as plausible targets for the SufABCDS iron-sulfur cluster assembly chaperone complex. Note that fold changes are listed after gene identification numbers. n.c., no change in expression.

binding motif found in *E. coli* K-12 ThiH is conserved in the *T. maritima* ThiH homolog (TM1267, 8.9-fold).

A connection to iron-sulfur cluster assembly is also apparent in the up-regulation of genes encoding enzymes involved in nicotinate biosynthesis (TM1643 to TM1645). *E. coli iscS* mutants have been shown to require NAD as well as thiamine, presumably due to defects in assembly of the iron-sulfur cluster of quinolinate synthetase, NadA (53). A NifS cysteine desulfurase homolog has also been shown to be required for NAD biosynthesis in *B. subtilis* (98). Increases in expression were observed here for genes encoding NadA (TM1644, 7.1-fold), NadC (TM1645, 8.1-fold), and an $NADP^+$-dependent L-aspartate dehydrogenase (TM1643, 27.9-fold) recently shown to convert L-aspartate to iminoaspartate (124) as an alternative to an NadB-type L-aspartate oxidase in the *T. maritima* NAD biosynthesis pathway. Increased NAD and/or NADH pools in sessile *T. maritima* may relate to the up-regulation of genes encoding L-lactate dehydrogenase (TM1867, 5.1-fold) (72), putative NADH oxidases (TM0379, 2.3-fold; TM0395, 3.5-fold), and the predicted dihydrolipoamide dehydrogenase (TM0381, 1.7-fold). L-Lactate dehydrogenase induction has also been observed in *B. cereus* biofilms (71) and may be involved in regenerating NAD^+ (66) in conjunction with NADH oxidases (38, 117).

Regulation of biofilm formation and maintenance. The genome sequence of *T. maritima* reveals the apparent lack of orthologs to a number of known biofilm-induced regulators, including RpoS, BmrAB, and CpsR. However, putative transcriptional regulators induced in sessile *T. maritima* cells included the sensor histidine kinase TM0187 (2.2-fold) and the response regulator TM1360 (1.6-fold). While the roles of these proteins have not yet been determined, the importance of a variety of related proteins in signaling processes during mesophilic biofilm formation has been well established (55). Small but statistically significant expression changes (1.8-fold) were also observed for TM0842, a CheY-related response regulator, and TM0841, a similarly regulated S-layer-like array protein sharing 35% identity (460 aa) with *Thermus thermophilus* SlpM (69), an activator of bacterial cell surface-layer protein synthesis.

Regulation of sigma factor expression influences biofilm formation in a number of species (1, 48). Little functional information is available for *T. maritima* sigma factors (13); however, the up-regulation of homologs to *sigA* (TM1451, 2.0-fold) and

sigE (TM1598, 1.6-fold) in biofilm cells hints at a possible role for these proteins as global regulators during *T. maritima* biofilm formation. In contrast, the only two other *T. maritima* sigma factor homologs, *sigH* (TM0534) and *fliA* (TM0902), showed little fluctuation in expression levels for the two conditions compared here. Putative regulatory proteins induced in biofilm cells included members of the LytR (TM1866, 2.3-fold), biotin repressor (TM1602, 2.4-fold), and AcrR/TetR (TM0823, 2.7-fold) families. None of these proteins has been characterized in *T. maritima*, although regulators with TetR DNA binding domains have previously been shown to be important in biofilm formation in mesophiles (17, 48).

No function is known for the predicted transcriptional regulator TM1602 (2.4-fold); however, the major facilitator superfamily permease (TM1603) bears sequence similarity to a *B. subtilis* transporter conferring resistance to the toxic oxyanion tellurite, $TeO_3^{(2^-)}$ (50) (Table 1). The IscS cysteine desulfurase and the CysK cysteine synthase of *Geobacillus stearothermophilis* also confer tellurite resistance on *E. coli* K-12, presumably protecting cells from superoxide-mediated iron-sulfur cluster degradation (102, 113). Complementation of a tellurite-hypersensitive *E. coli* K-12 *iscS* mutant with *G. stearothermophilus iscS* confers tellurite resistance and relieves a growth requirement for thiamine but not nicotinic acid (102). The isolation of a number of tellurite- and selenite-resistant strains of bacteria from hydrothermal vents near sulfide rocks and bacterial biofilms suggests that the expression changes observed here may indicate an adaptive response to an iron-sulfur cluster degradation stimulus in the natural environment of *T. maritima* (81).

Summary. The complex nature of biofilm formation processes, the dynamic physical and chemical characteristics of these microenvironments, and the likely heterogeneity of cellular states comprising biofilm populations make assigning a definitive biofilm phenotype difficult for *T. maritima*. Nonetheless, clear transcriptional differences were ascertained here that relate to cells involved in surface colonization. There is still much to be understood about biofilm formation and dynamics for *T. maritima*, but this work provides evidence for biofilm formation by *T. maritima*, a methodology for generating sufficient biofilm populations on nylon mesh in a high-temperature anaerobic chemostat for subsequent investigation of transcriptional response comparing planktonic and sessile cells, as well as a list of candidate genes whose expression patterns suggest a role in this process.

ACKNOWLEDGMENTS

This work was supported in part by grants from the National Science Foundation, NASA Exobiology Program, and the Department of Energy (Energy Biosciences Program). S.B.C. acknowledges support from an NIEHS Traineeship in Bioinformatics.

We thank M. Dykstra at the Electron Microscopy Center, NCSU School of Veterinary Medicine, for assistance with electron microscopy; and Stephanie Bridger, Ubie Sullivan, Jennifer Strayhorn, and Leon Kluskens for their assistance in generation of the PCR products used to construct the array. We also thank R. Wolfinger and K. Scott, SAS Institute, Cary, N.C., for help with implementing the mixed-model analysis and the NCSU Genome Research Laboratory for assistance with microarray development and use.

REFERENCES

1. **Adams, J. L., and R. J. C. McLean.** 1999. Impact of *rpoS* deletion on *Escherichia coli* biofilms. Appl. Environ. Microbiol. **65:**4285–4287.
2. **Andrews, S. C., A. K. Robinson, and F. Rodriguez-Quinones.** 2003. Bacterial iron homeostasis. FEMS Microbiol. Rev. **27:**215–237.
3. **Antón, J., I. Meseguer, and F. Rodriguez-Valera.** 1988. Production of an extracellular polysaccharide by *Haloferax mediterranei*. Appl. Environ. Microbiol. **54:**2381–2386.
4. **Arigoni, F., P. A. Kaminski, H. Hennecke, and C. Elmerich.** 1991. Nucleotide sequence of the *fixABC* region of *Azorhizobium caulinodans* ORS571: similarity of the *fixB* product with eukaryotic flavoproteins, characterization of *fixX*, and identification of *nifW*. Mol. Gen. Genet. **225:**514–520.
5. **Baaghil, S., A. Lewin, G. R. Moore, and N. E. Le Brun.** 2003. Core formation in *Escherichia coli* bacterioferritin requires a functional ferroxidase center. Biochemistry **42:**14047–14056.
6. **Beam, C. E., C. J. Saveson, and S. T. Lovett.** 2002. Role for *radA/sms* in recombination intermediate processing in *Escherichia coli*. J. Bacteriol. **184:**6836–6844.
7. **Beloin, C., J. Valle, P. Latour-Lambert, P. Faure, M. Kzreminski, D. Balestrino, J. A. Haagensen, S. Molin, G. Prensier, B. Arbeille, and J. M. Ghigo.** 2004. Global impact of mature biofilm lifestyle on *Escherichia coli* K-12 gene expression. Mol. Microbiol. **51:**659–674.
8. **Bertini, I., J. A. Cowan, C. Del Bianco, C. Luchinat, and S. S. Mansy.** 2003. *Thermotoga maritima* IscU. Structural characterization and dynamics of a new class of metallochaperone. J. Mol. Biol. **331:**907–924.
9. **Blake, P. R., J. B. Park, F. O. Bryant, S. Aono, J. K. Magnuson, E. Eccleston, J. B. Howard, M. F. Summers, and M. W. Adams.** 1991. Determinants of protein hyperthermostability: purification and amino acid sequence of rubredoxin from the hyperthermophilic archaebacterium *Pyrococcus furiosus* and secondary structure of the zinc adduct by NMR. Biochemistry **30:**10885–10895.
10. **Bollinger, N., D. J. Hassett, B. H. Iglewski, J. W. Costerton, and T. R. McDermott.** 2001. Gene expression in *Pseudomonas aeruginosa*: evidence of iron override effects on quorum sensing and biofilm-specific gene regulation. J. Bacteriol. **183:**1990–1996.
11. **Burns, D. M., and I. R. Beacham.** 1986. Nucleotide sequence and transcriptional analysis of the *E. coli ushA* gene, encoding periplasmic UDP-sugar hydrolase (5′-nucleotidase): regulation of the *ushA* gene, and the signal sequence of its encoded protein product. Nucleic Acids Res. **14:**4325–4342.
12. **Caldwell, D. E., and J. W. Costerton.** 1996. Are bacterial biofilms constrained to Darwin's concept of evolution through natural selection? Microbiol. SEM **12:**347–358.
13. **Camarero, J. A., A. Shekhtman, E. A. Campbell, M. Chlenov, T. M. Gruber, D. A. Bryant, S. A. Darst, D. Cowburn, and T. W. Muir.** 2002. Autoregulation of a bacterial sigma factor explored by using segmental isotopic labeling and NMR. Proc. Natl. Acad. Sci. USA **99:**8536–8541.
14. **Chhabra, S. R., K. R. Shockley, S. B. Conners, K. L. Scott, R. D. Wolfinger, and R. M. Kelly.** 2003. Mixed model analysis of carbohydrate-induced differential expression patterns in the hyperthermophilic bacterium *Thermotoga maritima*. J. Biol. Chem. **278:**7540–7552.
15. **Chhabra, S. R., K. R. Shockley, D. E. Ward, and R. M. Kelly.** 2002. Regulation of endo-acting glycosyl hydrolases in the hyperthermophilic bacterium *Thermotoga maritima* grown on glucan- and mannan-based polysaccharides. Appl. Environ. Microbiol. **68:**545–554.
16. **Clay, M. D., C. A. Cosper, F. E. Jenney, Jr., M. W. Adams, and M. K. Johnson.** 2003. Nitric oxide binding at the mononuclear active site of reduced *Pyrococcus furiosus* superoxide reductase. Proc. Natl. Acad. Sci. USA **100:**3796–3801.
17. **Conlon, K. M., H. Humphreys, and J. P. O'Gara.** 2002. *icaR* encodes a transcriptional repressor involved in environmental regulation of *ica* operon expression and biofilm formation in *Staphylococcus epidermidis*. J. Bacteriol. **184:**4400–4408.
18. **Dakhova, O. N., N. E. Kurepina, V. V. Zverlov, V. A. Svetlichnyi, and G. A. Velikodvorskaya.** 1993. Cloning and expression in *Escherichia coli* of *Thermotoga neapolitana* genes coding for enzymes of carbohydrate substrate degradation. Biochem. Biophys. Res. Commun. **194:**1359–1364.
19. **Davies, D. G., A. M. Chakrabarty, and G. G. Geesey.** 1993. Exopolysaccharide production in biofilms: substratum activation of alginate gene expression by *Pseudomonas aeruginosa*. Appl. Environ. Microbiol. **59:**1181–1186.
20. **Davies, D. G., and G. G. Geesey.** 1995. Regulation of the alginate biosynthesis gene *algC* in *Pseudomonas aeruginosa* during biofilm development in continuous culture. Appl. Environ. Microbiol. **61:**860–867.
21. **Day, M. W., B. T. Hsu, L. Joshua-Tor, J. B. Park, Z. H. Zhou, M. W. Adams, and D. C. Rees.** 1992. X-ray crystal structures of the oxidized and reduced forms of the rubredoxin from the marine hyperthermophilic archaebacterium *Pyrococcus furiosus*. Protein Sci. **1:**1494–1507.
22. **Domingues, M. R., J. C. Araujo, M. B. A. Varesche, and R. F. Vazoller.** 2002. Evaluation of thermophilic anaerobic microbial consortia using fluorescence *in situ* hybridization (FISH). Water Sci. Technol. **45:**27–33.
23. **Donald, R. G. K., D. W. Nees, C. K. Raymond, A. I. Loroch, and R. A. Ludwig.** 1986. Characterization of three genomic loci encoding *Rhizobium* sp. strain ORS571 N_2 fixation genes. J. Bacteriol. **165:**72–81.
24. **Donlan, R. M.** 2000. Biofilm control in industrial water systems: approaching an old problem in new ways, p. 333–360. *In* L. V. Evans (ed.), Biofilms:

recent advances in their study and control. Harwood Academic Publishers, Singapore.
25. **Eichhorn, E., J. R. van der Ploeg, and T. Leisinger.** 2000. Deletion analysis of the *Escherichia coli* taurine and alkanesulfonate transport systems. J. Bacteriol. **182:**2687–2695.
26. **Fiegler, H., and R. Bruckner.** 1997. Identification of the serine acetyltransferase gene of *Staphylococcus xylosus*. FEMS Microbiol. Lett. **148:**181–187.
27. **Frazao, C., G. Silva, C. M. Gomes, P. Matias, R. Coelho, L. Sieker, S. Macedo, M. Y. Liu, S. Oliveira, M. Teixeira, A. V. Xavier, C. Rodrigues-Pousada, M. A. Carrondo, and J. Le Gall.** 2000. Structure of a dioxygen reduction enzyme from *Desulfovibrio gigas*. Nat. Struct. Biol. **7:**1041–1045.
28. **Ghigo, J. M.** 2003. Are there biofilm-specific physiological pathways beyond a reasonable doubt? Res. Microbiol. **154:**1–8.
29. **Golovlev, E. L.** 2002. The mechanism of formation of *Pseudomonas aeruginosa* biofilm, a type of structured population. Microbiology **71:**249–254.
30. **Gronger, P., S. S. Manian, H. Reilander, M. O'Connell, U. B. Priefer, and A. Puhler.** 1987. Organization and partial sequence of a DNA region of the *Rhizobium leguminosarum* symbiotic plasmid pRL6JI containing the genes *fixABC*, *nifA*, *nifB* and a novel open reading frame. Nucleic Acids Res. **15:**31–49.
31. **Guezennec, J.** 1999. Microbial exopolysaccharides from extreme environments. Agro Food Ind. Hi-Tech **10:**34–35.
32. **Guo, R. T., C. J. Kuo, C. C. Chou, T. P. Ko, H. L. Shr, P. H. Liang, and A. H. Wang.** 2004. Crystal structure of octaprenyl pyrophosphate synthase from hyperthermophilic *Thermotoga maritima* and mechanism of product chain length determination. J. Biol. Chem. **279:**4903–4912.
33. **Hantke, K.** 2003. Is the bacterial ferrous iron transporter FeoB a living fossil? Trends Microbiol. **11:**192–195.
34. **Hasseman, J.** 2001. TIGR microarray protocols. [Online.] http://www.tigr.org/tdb/microarray/protocolsTIGR.shtml.
35. **Hinsa, S. M., M. Espinosa-Urgel, J. L. Ramos, and G. A. O'Toole.** 2003. Transition from reversible to irreversible attachment during biofilm formation by *Pseudomonas fluorescens* WCS365 requires an ABC transporter and a large secreted protein. Mol. Microbiol. **49:**905–918.
36. **Hirata, H., T. Fukazawa, S. Negoro, and H. Okada.** 1986. Structure of a β-galactosidase gene of *Bacillus stearothermophilus*. J. Bacteriol. **166:**722–727.
37. **Huber, R., T. A. Langworthy, H. Konig, M. Thomm, C. R. Woese, U. B. Sleytr, and K. O. Stetter.** 1986. *Thermotoga maritima* sp. nov. represents a new genus of unique extremely thermophilic eubacteria growing up to 90°C. Arch. Microbiol. **144:**324–333.
38. **Jenney, F., M. Verhage, X. Cui, and M. W. W. Adams.** 1999. Anaerobic microbes: oxygen detoxification without superoxide dismutase. Science **286:**306–309.
39. **Jeong, W., M. K. Cha, and I. H. Kim.** 2000. Thioredoxin-dependent hydroperoxide peroxidase activity of bacterioferritin comigratory protein (BCP) as a new member of the thiol-specific antioxidant protein (TSA)/alkyl hydroperoxide peroxidase C (AhpC) family. J. Biol. Chem. **275:**2924–2930.
40. **Kacklany, S. C., S. B. Levery, J. S. Kim, B. L. Reuhs, L. W. Lion, and W. C. Ghiorse.** 2001. Structure and carbohydrate analysis of the exopolysaccharide capsule of *Pseudomonas putida* G7. Environ. Microbiol. **3:**774–784.
41. **Kaiser, J. T., T. Clausen, G. P. Bourenkow, H. D. Bartunik, S. Steinbacher, and R. Huber.** 2000. Crystal structure of a NifS-like protein from *Thermotoga maritima*: implications for iron sulphur cluster assembly. J. Mol. Biol. **297:**451–464.
42. **Kaminski, P. A., F. Norel, N. Desnoues, A. Kush, G. Salzano, and C. Elmerich.** 1988. Characterization of the *fixABC* region of *Azorhizobium caulinodans* ORS571 and identification of a new nitrogen fixation gene. Mol. Gen. Genet. **214:**496–502.
43. **Kammler, M., C. Schön, and K. Hantke.** 1993. Characterization of the ferrous iron uptake system of *Escherichia coli*. J. Bacteriol. **175:**6212–6219.
44. **Kashima, Y., and K. Ishikawa.** 2003. Alkyl hydroperoxide reductase dependent on thioredoxin-like protein from *Pyrococcus horikoshii*. J. Biochem. (Tokyo) **134:**25–29.
45. **Kashiwagi, K., S. Miyamoto, E. Nukui, H. Kobayashi, and K. Igarashi.** 1993. Functions of PotA and PotD proteins in spermidine-preferential uptake system in *Escherichia coli*. J. Biol. Chem. **268:**19358–19363.
46. **Kim, D. Y., D. R. Kim, S. C. Ha, N. K. Lokanath, C. J. Lee, H. Y. Hwang, and K. K. Kim.** 2003. Crystal structure of the protease domain of a heat-shock protein HtrA from *Thermotoga maritima*. J. Biol. Chem. **278:**6543–6551.
47. **Kim, D. Y., and K. K. Kim.** 2002. Crystallization and preliminary X-ray studies of the protease domain of the heat-shock protein HtrA from *Thermotoga maritima*. Acta Crystallogr. D Biol. Crystallogr. **58:**170–172.
48. **Kojic, M., and V. Venturi.** 2001. Regulation of *rpoS* gene expression in *Pseudomonas*: involvement of a TetR family regulator. J. Bacteriol. **183:**3712–3720.
49. **Kolter, R., and R. Losick.** 1998. One for all and all for one. Science **280:**226–227.
50. **Kumano, M., A. Tamakoshi, and K. Yamane.** 1997. A 32 kb nucleotide sequence from the region of the lincomycin-resistance gene (22°-25°) of the *Bacillus subtilis* chromosome and identification of the site of the lin-2 mutation. Microbiology **143:**2775–2782.
51. **Kuo, T. H., and P. H. Liang.** 2002. Reaction kinetic pathway of the recombinant octaprenyl pyrophosphate synthase from *Thermotoga maritima*: how is it different from that of the mesophilic enzyme. Biochim. Biophys. Acta **1599:**125–133.
52. **LaPaglia, C., and P. L. Hartzell.** 1997. Stress-induced production of biofilm in the hyperthermophile *Archaeoglobus fulgidus*. Appl. Environ. Microbiol. **63:**3158–3163.
53. **Lauhon, C. T., and R. Kambampati.** 2000. The *iscS* gene in *Escherichia coli* is required for the biosynthesis of 4-thiouridine, thiamin, and NAD. J. Biol. Chem. **275:**20096–20103.
54. **Lee, M. H., Y. W. Kim, T. J. Kim, C. S. Park, J. W. Kim, T. W. Moon, and K. H. Park.** 2002. A novel amylolytic enzyme from *Thermotoga maritima*, resembling cyclodextrinase and alpha-glucosidase, that liberates glucose from the reducing end of the substrates. Biochem. Biophys. Res. Commun. **295:**818–825.
55. **Lejeune, P.** 2003. Contamination of abiotic surfaces: what a colonizing bacterium sees and how to blur it. Trends Microbiol. **11:**179–184.
56. **Leonardi, R., S. A. Fairhurst, M. Kriek, D. J. Lowe, and P. L. Roach.** 2003. Thiamine biosynthesis in *Escherichia coli*: isolation and initial characterisation of the ThiGH complex. FEBS Lett. **539:**95–99.
57. **Liebl, W., P. Ruile, K. Bronnenmeier, K. Riedel, F. Lottspeich, and I. Greif.** 1996. Analysis of a *Thermotoga maritima* DNA fragment encoding two similar thermostable cellulases, CelA and CelB, and characterization of the recombinant enzymes. Microbiology **142:**2533–2542.
58. **Mansy, S. S., G. Wu, K. K. Surerus, and J. A. Cowan.** 2002. Iron-sulfur cluster biosynthesis. *Thermotoga maritima* IscU is a structured iron-sulfur cluster assembly protein. J. Biol. Chem. **277:**21397–21404.
59. **Mansy, S. S., S. P. Wu, and J. A. Cowan.** 2004. Iron-sulfur cluster biosynthesis: biochemical characterization of the conformational dynamics of *Thermotoga maritima* IscU and the relevance for cellular cluster assembly. J. Biol. Chem. **279:**10469–10475.
60. **Marlovits, T. C., W. Haase, C. Herrmann, S. G. Aller, and V. M. Unger.** 2002. The membrane protein FeoB contains an intramolecular G protein essential for Fe(II) uptake in bacteria. Proc. Natl. Acad. Sci. USA **99:**16243–16248.
61. **Masepohl, B., F. Fuhrer, and W. Klipp.** 2001. Genetic analysis of a *Rhodobacter capsulatus* gene region involved in utilization of taurine as a sulfur source. FEMS Microbiol. Lett. **205:**105–111.
62. **Michelini, E. T., and G. C. Flynn.** 1999. The unique chaperone operon of *Thermotoga maritima*: cloning and initial characterization of a functional Hsp70 and small heat shock protein. J. Bacteriol. **181:**4237–4244.
63. **Muralidharan, V., K. D. Rinker, I. S. Hirsh, E. J. Bouwer, and R. M. Kelly.** 1997. Hydrogen transfer between methanogens and fermentative heterotrophs in hyperthermophilic cocultures. Biotechnol. Bioeng. **56:**268–278.
64. **Nachin, L., L. Loiseau, D. Expert, and F. Barras.** 2003. SufC: an unorthodox cytoplasmic ABC/ATPase required for [Fe-S] biogenesis under oxidative stress. EMBO J. **22:**427–437.
65. **Nelson, K. E., R. A. Clayton, S. R. Gill, M. L. Gwinn, R. J. Dodson, D. H. Haft, E. K. Hickey, L. D. Peterson, W. C. Nelson, K. A. Ketchum, L. McDonald, T. R. Utterback, J. A. Malek, K. D. Linher, M. M. Garrett, A. M. Stewart, M. D. Cotton, M. S. Pratt, C. A. Phillips, D. Richardson, J. Heidelberg, G. G. Sutton, R. D. Fleischmann, J. A. Eisen, O. White, S. L. Salzberg, H. O. Smith, J. C. Venter, and C. M. Fraser.** 1999. Evidence for lateral gene transfer between Archaea and Bacteria from genome sequence of *Thermotoga maritima*. Nature **399:**323–329.
66. **Neves, A. R., R. Ventura, N. Mansour, C. Shearman, M. J. Gasson, C. Maycock, A. Ramos, and H. Santos.** 2002. Is the glycolytic flux in *Lactococcus lactis* primarily controlled by the redox charge? Kinetics of NAD+ and NADH pools determined by ^{13}C NMR. J. Biol. Chem. **277:**28088–28098.
67. **Nicolaus, B., M. C. Manca, I. Romano, and L. Lama.** 1993. Production of an exopolysaccharide from two thermophilic archaea belonging to the genus *Sulfolobus*. FEMS Microbiol. Lett. **109:**203–206.
68. **Nidetzky, B., C. Eis, and M. Albert.** 2000. Role of non-covalent enzyme-substrate interactions in the reaction catalysed by cellobiose phosphorylase from *Cellulomonas uda*. Biochem. J. **351:**649–659.
69. **Olabarria, G., L. A. Fernandez-Herrero, J. L. Carrascosa, and J. Berenguer.** 1996. *slpM*, a gene coding for an "S-layer-like array" overexpressed in S-layer mutants of *Thermus thermophilus* HB8. J. Bacteriol. **178:**357–365.
70. **Ollagnier-de-Choudens, S., D. Lascoux, L. Loiseau, F. Barras, E. Forest, and M. Fontecave.** 2003. Mechanistic studies of the SufS-SufE cysteine desulfurase: evidence for sulfur transfer from SufS to SufE. FEBS Lett. **555:**263–267.
71. **Oosthuizen, M. C., B. Steyn, J. Theron, P. Cosette, D. Lindsay, A. von Holy, and V. S. Brözel.** 2002. Proteomic analysis reveals differential protein expression by *Bacillus cereus* during biofilm formation. Appl. Environ. Microbiol. **68:**2770–2780.
72. **Ostendorp, R., W. Liebl, H. Schurig, and R. Jaenicke.** 1993. The L-lactate dehydrogenase gene of the hyperthermophilic bacterium *Thermotoga ma-*

ritima cloned by complementation in *Escherichia coli*. Eur. J. Biochem. **216:**709–715.
73. **O'Toole, G. A., and R. Kolter.** 1998. Initiation of biofilm formation in *Pseudomonas fluorescens* WCS365 proceeds via multiple, convergent signalling pathways: a genetic analysis. Mol. Microbiol. **28:**449–461.
74. **Pan, G., A. L. Menon, and M. W. Adams.** 2003. Characterization of a [2Fe-2S] protein encoded in the iron-hydrogenase operon of *Thermotoga maritima*. J. Biol. Inorg. Chem. **8:**469–474.
75. **Park, S., and J. A. Imlay.** 2003. High levels of intracellular cysteine promote oxidative DNA damage by driving the Fenton reaction. J. Bacteriol. **185:** 1942–1950.
76. **Phadtare, S., J. Hwang, K. Severinov, and M. Inouye.** 2003. CspB and CspL, thermostable cold-shock proteins from *Thermotoga maritima*. Genes Cells **8:**801–810.
77. **Pysz, M. A., K. D. Rinker, K. R. Shockley, and R. M. Kelly.** 2001. Continuous cultivation of hyperthermophiles. Hyperthermophilic Methods Enzymol. **330:**31–40.
78. **Pysz, M. A., D. E. Ward, K. R. Shockley, C. I. Montero, S. B. Conners, M. R. Johnson, and R. M. Kelly.** 2004. Transcriptional analysis of dynamic heat-shock response by the hyperthermophilic bacterium *Thermotoga maritima.* Extremophiles **8:**209–217.
79. **Rajashekhara, E., M. Kitaoka, Y. K. Kim, and K. Hayashi.** 2002. Characterization of a cellobiose phosphorylase from a hyperthermophilic eubacterium, *Thermotoga maritima* MSB8. Biosci. Biotechnol. Biochem. **66:**2578–2586.
80. **Rangachari, K., C. T. Davis, J. F. Eccleston, E. M. Hirst, J. W. Saldanha, M. Strath, and R. J. Wilson.** 2002. SufC hydrolyzes ATP and interacts with SufB from *Thermotoga maritima*. FEBS Lett. **514:**225–228.
81. **Rathgeber, C., N. Yurkova, E. Stackebrandt, J. T. Beatty, and V. Yurkov.** 2002. Isolation of tellurite- and selenite-resistant bacteria from hydrothermal vents of the Juan de Fuca Ridge in the Pacific Ocean. Appl. Environ. Microbiol. **68:**4613–4622.
82. **Ravasio, S., B. Curti, and M. A. Vanoni.** 2001. Determination of the midpoint potential of the FAD and FMN flavin cofactors and of the 3Fe-4S cluster of glutamate synthase. Biochemistry **40:**5533–5541.
83. **Reysenbach, A. L., and E. Shock.** 2002. Merging genomes with geochemistry in hydrothermal ecosystems. Science **296:**1077–1082.
84. **Rinker, K. D.** 1998. Growth physiology and bioenergetics of the hyperthermophilic archaeon *Thermococcus litoralis* and bacterium *Thermotoga maritima.* Ph.D. thesis. North Carolina State University, Raleigh.
85. **Rinker, K. D., C. J. Han, and R. M. Kelly.** 1999. Continuous culture as a tool for investigating the growth physiology of heterotrophic hyperthermophiles and extreme thermoacidophiles. J. Appl. Microbiol. **85:**118–127.
86. **Rinker, K. D., and R. M. Kelly.** 2000. Effect of carbon and nitrogen sources on growth dynamics and exopolysaccharide production for the hyperthermophilic archaeon *Thermococcus litoralis* and bacterium *Thermotoga maritima*. Biotechnol. Bioeng. **69:**537–547.
87. **Rinker, K. D., and R. M. Kelly.** 1996. Growth physiology of the hyperthermophilic archaeon *Thermococcus litoralis*: development of a sulfur-free defined medium, characterization of an exopolysaccharide, and evidence of biofilm formation. Appl. Environ. Microbiol. **62:**4478–4485.
88. **Sauer, K.** 27 May 2003, posting date. The genomics and proteomics of biofilm formation. Genome Biol. **4:**219. [Online.] http://genomebiology-.com.
89. **Sauer, K., and A. K. Camper.** 2001. Characterization of phenotypic changes in *Pseudomonas putida* in response to surface-associated growth. J. Bacteriol. **183:**6579–6589.
90. **Sauer, K., A. K. Camper, G. D. Ehrlich, J. W. Costerton, and D. G. Davies.** 2002. *Pseudomonas aeruginosa* displays multiple phenotypes during development as a biofilm. J. Bacteriol. **184:**1140–1154.
91. **Schembri, M. A., K. Kjaergaard, and P. Klemm.** 2003. Global gene expression in *Escherichia coli* biofilms. Mol. Microbiol. **48:**253–267.
92. **Schwartz, C. J., J. L. Giel, T. Patschkowski, C. Luther, F. J. Ruzicka, H. Beinert, and P. J. Kiley.** 2001. IscR, an Fe-S cluster-containing transcription factor, represses expression of *Escherichia coli* genes encoding Fe-S cluster assembly proteins. Proc. Natl. Acad. Sci. USA **98:**14895–14900.
93. **Sharma, R., C. Rensing, B. P. Rosen, and B. Mitra.** 2000. The ATP hydrolytic activity of purified ZntA, a Pb(II)/Cd(II)/Zn(II)-translocating ATPase from *Escherichia coli*. J. Biol. Chem. **275:**3873–3878.
94. **Snel, B., G. Lehmann, P. Bork, and M. A. Huynen.** 2000. STRING: a web-server to retrieve and display the repeatedly occurring neighbourhood of a gene. Nucleic Acids Res. **28:**3442–3444.
95. **Stearman, R., D. S. Yuan, Y. Yamaguchi-Iwai, R. D. Klausner, and A. Dancis.** 1996. A permease-oxidase complex involved in high-affinity iron uptake in yeast. Science **271:**1552–1557.
96. **Stoodley, P., K. Sauer, D. G. Davies, and J. W. Costerton.** 2002. Biofilms as complex differentiated communities. Annu. Rev. Microbiol. **56:**187–209.
97. **Storz, G., and J. A. Imlay.** 1999. Oxidative stress. Curr. Opin. Microbiol. **2:**188–194.
98. **Sun, D., and P. Setlow.** 1993. Cloning, nucleotide sequence, and regulation of the *Bacillus subtilis nadB* gene and a *nifS*-like gene, both of which are essential for NAD biosynthesis. J. Bacteriol. **175:**1423–1432.
99. **Suresh, C., M. Kitaoka, and K. Hayashi.** 2003. A thermostable non-xylanolytic alpha-glucuronidase of *Thermotoga maritima* MSB8. Biosci. Biotechnol. Biochem. **67:**2359–2364.
100. **Svensater, G., J. Welin, J. C. Wilkins, D. Beighton, and I. R. Hamilton.** 2001. Protein expression by planktonic and biofilm cells of *Streptococcus mutans*. FEMS Microbiol. Lett. **205:**139–146.
101. **Takahashi, Y., and U. Tokumoto.** 2002. A third bacterial system for the assembly of iron-sulfur clusters with homologs in archaea and plastids. J. Biol. Chem. **277:**28380–28383.
102. **Tantaleán, J. C., M. A. Araya, C. P. Saavedra, D. E. Fuentes, J. M. Pérez, I. L. Calderón, P. Youderian, and C. C. Vásquez.** 2003. The *Geobacillus stearothermophilus* V *iscS* gene, encoding cysteine desulfurase, confers resistance to potassium tellurite in *Escherichia coli* K-12. J. Bacteriol. **185:** 5831–5837.
103. **Tao, X., R. Khayat, D. Christendat, A. Savchenko, X. Xu, S. Goldsmith-Fischman, B. Honig, A. Edwards, C. H. Arrowsmith, and L. Tong.** 2003. Crystal structures of MTH1187 and its yeast ortholog YBL001c. Proteins **52:**478–480.
104. **Taylor, S. V., N. L. Kelleher, C. Kinsland, H. J. Chiu, C. A. Costello, A. D. Backstrom, F. W. McLafferty, and T. P. Begley.** 1998. Thiamin biosynthesis in *Escherichia coli*. Identification of this thiocarboxylate as the immediate sulfur donor in the thiazole formation. J. Biol. Chem. **273:**16555–16560.
105. **Tolker-Nielsen, T., U. C. Brinch, P. C. Ragas, J. B. Andersen, C. S. Jacobsen, and S. Molin.** 2000. Development and dynamics of *Pseudomonas* sp. biofilms. J. Bacteriol. **182:**6482–6489.
106. **Tremoulet, F., O. Duche, A. Namane, B. Martinie, and J. C. Labadie.** 2002. A proteomic study of *Escherichia coli* O157:H7 NCTC 12900 cultivated in biofilm or in planktonic growth mode. FEMS Microbiol. Lett. **215:**7–14.
107. **Tremoulet, F., O. Duche, A. Namane, B. Martinie, The European** *Listeria* Genome Consortium, and J. C. Labadie. 2002. Comparison of protein patterns of *Listeria monocytogenes* grown in biofilm or in planktonic mode by proteome analysis. FEMS Microbiol. Lett. **210:**25–31.
108. **Ugulava, N. B., B. R. Gibney, and J. T. Jarrett.** 2001. Biotin synthase contains two distinct iron-sulfur cluster binding sites: chemical and spectroelectrochemical analysis of iron-sulfur cluster interconversions. Biochemistry **40:**8343–8351.
109. **Valdes-Stauber, N., and S. Scherer.** 1996. Nucleotide sequence and taxonomical distribution of the bacteriocin gene *lin* cloned from *Brevibacterium linens* M18. Appl. Environ. Microbiol. **62:**1283–1286.
110. **van der Ploeg, J. R., R. Iwanicka-Nowicka, T. Bykowski, M. M. Hryniewicz, and T. Leisinger.** 1999. The *Escherichia coli ssuEADCB* gene cluster is required for the utilization of sulfur from aliphatic sulfonates and is regulated by the transcriptional activator Cbl. J. Biol. Chem. **274:**29358–29365.
111. **van der Ploeg, J. R., M. A. Weiss, E. Saller, H. Nashimoto, N. Saito, M. A. Kertesz, and T. Leisinger.** 1996. Identification of sulfate starvation-regulated genes in *Escherichia coli*: a gene cluster involved in the utilization of taurine as a sulfur source. J. Bacteriol. **178:**5438–5446.
112. **van Kranenburg, R., H. R. Vos, I. I. van Swam, M. Kleerebezem, and W. M. de Vos.** 1999. Functional analysis of glycosyltransferase genes from *Lactococcus lactis* and other gram-positive cocci: complementation, expression, and diversity. J. Bacteriol. **181:**6347–6353.
113. **Vasquez, C. C., C. P. Saavedra, C. A. Loyola, M. A. Araya, and S. Pichuantes.** 2001. The product of the *cysK* gene of *Bacillus stearothermophilus* V mediates potassium tellurite resistance in *Escherichia coli*. Curr. Microbiol. **43:**418–423.
114. **Verhagen, M. F., T. O'Rourke, and M. W. Adams.** 1999. The hyperthermophilic bacterium, *Thermotoga maritima*, contains an unusually complex iron-hydrogenase: amino acid sequence analyses versus biochemical characterization. Biochim. Biophys. Acta **1412:**212–229.
115. **Wakagi, T.** 2003. Sulerythrin, the smallest member of the rubrerythrin family, from a strictly aerobic and thermoacidophilic archaeon, *Sulfolobus tokodaii* strain 7. FEMS Microbiol. Lett. **222:**33–37.
116. **Walt, A., and M. L. Kahn.** 2002. The *fixA* and *fixB* genes are necessary for anaerobic carnitine reduction in *Escherichia coli*. J. Bacteriol. **184:**4044–4047.
117. **Ward, D. E., C. J. Donnelly, M. E. Mullendore, J. van der Oost, W. M. de Vos, and E. J. Crane.** 2001. The NADH oxidase from *Pyrococcus furiosus*. Implications for the protection of anaerobic hyperthermophiles against oxidative stress. Eur. J. Biochem. **268:**5816–5823.
118. **Wassenberg, D., W. Liebl, and R. Jaenicke.** 2000. Maltose-binding protein from the hyperthermophilic bacterium *Thermotoga maritima*: stability and binding properties. J. Mol. Biol. **295:**279–288.
119. **Watnick, P., and R. Kolter.** 2000. Biofilm, city of microbes. J. Bacteriol. **182:**2675–2679.
120. **Welker, C., G. Bohm, H. Schurig, and R. Jaenicke.** 1999. Cloning, overexpression, purification, and physicochemical characterization of a cold shock protein homolog from the hyperthermophilic bacterium *Thermotoga maritima*. Protein Sci. **8:**394–403.
121. **Whiteley, M., M. G. Bangera, R. E. Bumgarner, M. R. Parsek, G. M.**

Teitzel, S. Lory, and E. P. Greenberg. 2001. Gene expression in *Pseudomonas aeruginosa* biofilms. Nature **413:**860–864.

122. **Wolfinger, R. D., G. Gibson, E. D. Wolfinger, L. Bennett, H. Hamadeh, P. Bushel, C. Afshari, and R. S. Paules.** 2001. Assessing gene significance from cDNA microarray expression data via mixed models. J. Comput. Biol. **8:**625–637.
123. **Yan, L., K. G. Boyd, D. R. Adams, and J. G. Burgess.** 2003. Biofilm-specific cross-species induction of antimicrobial compounds in bacilli. Appl. Environ. Microbiol. **69:**3719–3727.
124. **Yang, Z., A. Savchenko, A. Yakunin, R. Zhang, A. Edwards, C. Arrowsmith, and L. Tong.** 2003. Aspartate dehydrogenase, a novel enzyme identified from structural and functional studies of TM1643. J. Biol. Chem. **278:**8804–8808.
125. **Yeh, A. P., Y. Hu, F. E. Jenney, Jr., M. W. Adams, and D. C. Rees.** 2000. Structures of the superoxide reductase from *Pyrococcus furiosus* in the oxidized and reduced states. Biochemistry **39:**2499–2508.
126. **Yernool, D. A., J. K. McCarthy, D. E. Eveleigh, and J. D. Bok.** 2000. Cloning and characterization of the glucooligosaccharide catabolic pathway β-glucan glucohydrolase and cellobiose phosphorylase in the marine hyperthermophile *Thermotoga neapolitana*. J. Bacteriol. **182:**5172–5179.
127. **Yildiz, F. H., and G. K. Schoolnik.** 1999. *Vibrio cholerae* O1 El Tor: identification of a gene cluster required for the rugose colony type, exopolysaccharide production, chlorine resistance, and biofilm formation. Proc. Natl. Acad. Sci. USA **96:**4028–4033.
128. **Yu, H., M. J. Schurr, and V. Deretic.** 1995. Functional equivalence of *Escherichia coli* σ^E and *Pseudomonas aeruginosa* AlgU: *E. coli rpoE* restores mucoidy and reduces sensitivity to reactive oxygen intermediates in *algU* mutants of *P. aeruginosa*. J. Bacteriol. **177:**3259–3268.